Journal of Medicinal Chemistry

Article

Cite This: J. Med. Chem. 2018, 61, 3059−3075

pubs.acs.org/jmc

Further Developments of the Phenyl-Pyrrolyl Pentane Series of Nonsteroidal Vitamin D Receptor Modulators as Anticancer Agents

Meixi Hao,[†] Siyuan Hou,[†] Lingjing Xue, Haoliang Yuan, Lulu Zhu, Cong Wang, Bin Wang, Chunming Tang, and Can Zhang*

State Key Laboratory of Natural Medicines and Jiangsu Key Laboratory of Drug Discovery for Metabolic Diseases, Center of Drug Discovery, China Pharmaceutical University, 24 Tong Jia Xiang, Nanjing 210009, China

Supporting Information

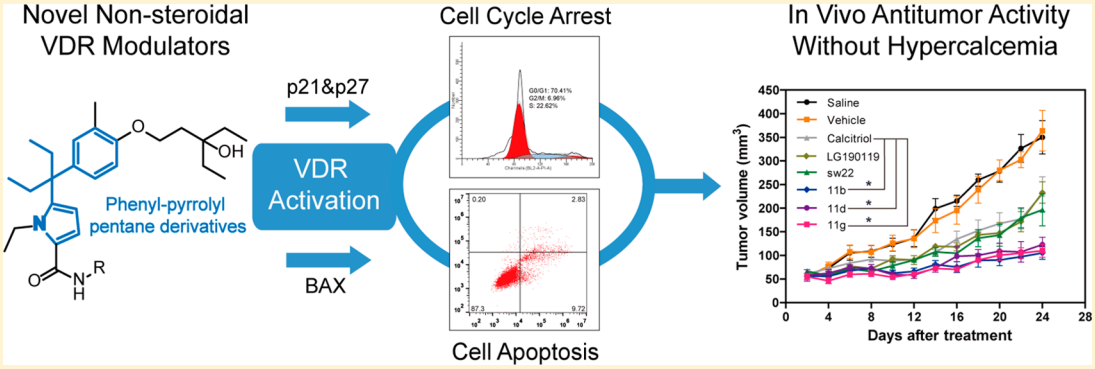

ABSTRACT: The vitamin D_3 receptor (VDR), which belongs to the nuclear-receptor superfamily, is a potential molecular target for anticancer-drug discovery. In this study, a series of nonsteroidal vitamin D mimics with phenyl-pyrrolyl pentane skeletons with therapeutic potentials in cancer treatment were synthesized. Among them, **11b** and **11g** were identified as the most effective agents in reducing the viability of four cancer-cell lines, particularly those of breast-cancer cells, with IC_{50} values in the submicromolar-concentration range. In addition, **11b** and **11g** possessed VDR-binding affinities and displayed significant partial VDR-agonistic activities determined by dual-luciferase-reporter assays and human-leukemia-cell-line (HL-60)-differentiation assays. Furthermore, **11b** and **11g** inhibited tumor growth in an orthotopic breast-tumor model via inhibition of cell proliferation and induction of cell apoptosis. More importantly, **11b** and **11g** exhibited favorable pharmacokinetic behavior in vivo and did not increase serum calcium levels or cause any other apparent side effects. In summary, **11b** and **11g** act as novel VDR modulators and may be promising candidates for cancer chemotherapy.

INTRODUCTION

The active form of vitamin D_3, 1,25-dihydroxyvitamin D_3 (calcitriol, 1,25-$(OH)_2D_3$), regulates multiple signaling pathways by binding to its intracellular receptor, the vitamin D_3 receptor (VDR), which belongs to the nuclear-receptor superfamily of steroid hormones. Calcitriol and its synthetic analogues play important roles in calcium homeostasis, bone mineralization, and immune regulation.[1−3] However, over the past two decades, it has become clear that calcitriol and its analogues might have therapeutic potentials as anticancer agents by modulating the proliferation, apoptosis, and differentiation of a variety of cancer-cell types through the VDR-signaling pathway.[4,5]

Preclinical research indicates that vitamin D deficiencies raise the risk of developing cancers, such as colon cancer,[6,7] breast cancer,[8,9] and prostate cancer,[10,11] whereas dietary calcitriol and its analogues result in significant inhibitions of tumor growth and eventual tumor burden.[12,13] Additionally, *Vdr*-null mice are more sensitive to carcinogen-induced tumorigenesis.[14] More importantly, clinical studies further support the development of vitamin D modulators as preventative and therapeutic anticancer agents. Garland et al. discovered that exposure to sufficient sunlight could induce enough vitamin D_3 to reduce the mortality risks of patients with colon cancer.[15] Lappe et al. also discovered that improving calcium and vitamin D nutritional statuses substantially reduced cancer risks in postmenopausal women.[16] Moreover, seocalcitol, a vitamin D_3 analogue, displayed antitumor activity in the treatment of hepatocellular carcinoma (HCC) in a phase II trial study.[17] Combinational therapies with calcitriol and other anticancer agents improved the survival of prostate-cancer patients in phase II trials.[18,19] Therefore, it is essential to develop vitamin D modulators as preventative and therapeutic anticancer agents.

During the last 30 years, a large number of vitamin D analogues have been synthesized by introducing different types of chemical modifications to calcitriol, such as maxacalcitol, calcipotriol, seocalcitol, and lexicalcitol, which have been used

Received: January 22, 2018
Published: March 8, 2018

DOI: 10.1021/acs.jmedchem.8b00106
J. Med. Chem. 2018, 61, 3059−3075

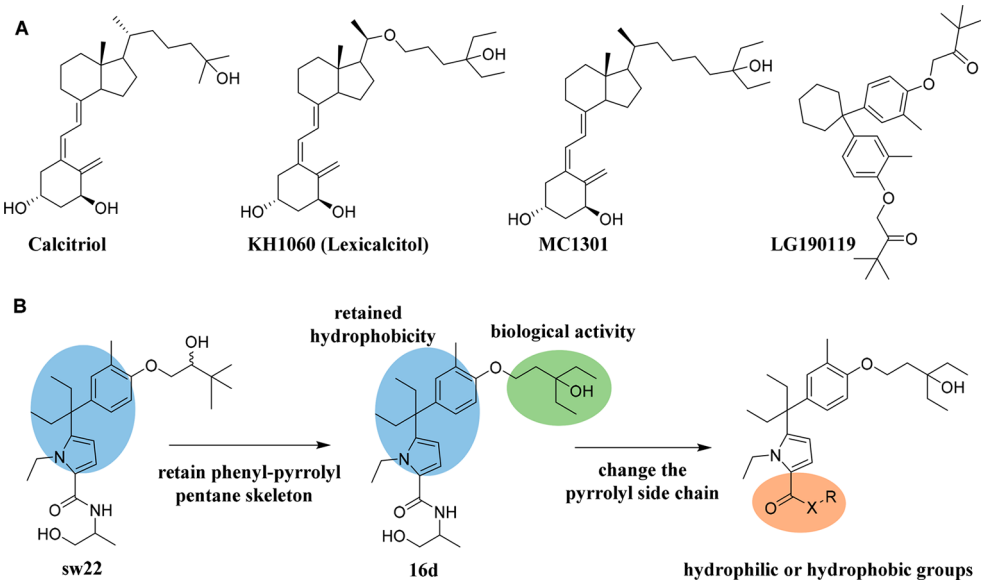

Figure 1. Designed VDR modulators. (A) Structures of calcitriol, lexicalcitol, MC1301, and LG190119. (B) Design of nonsteroidal VDR modulators with phenyl-pyrrolyl pentane skeletons.

Scheme 1. Synthesis of the Phenyl-Pyrrolyl Pentane Series of Nonsteroidal VDR Derivatives[a]

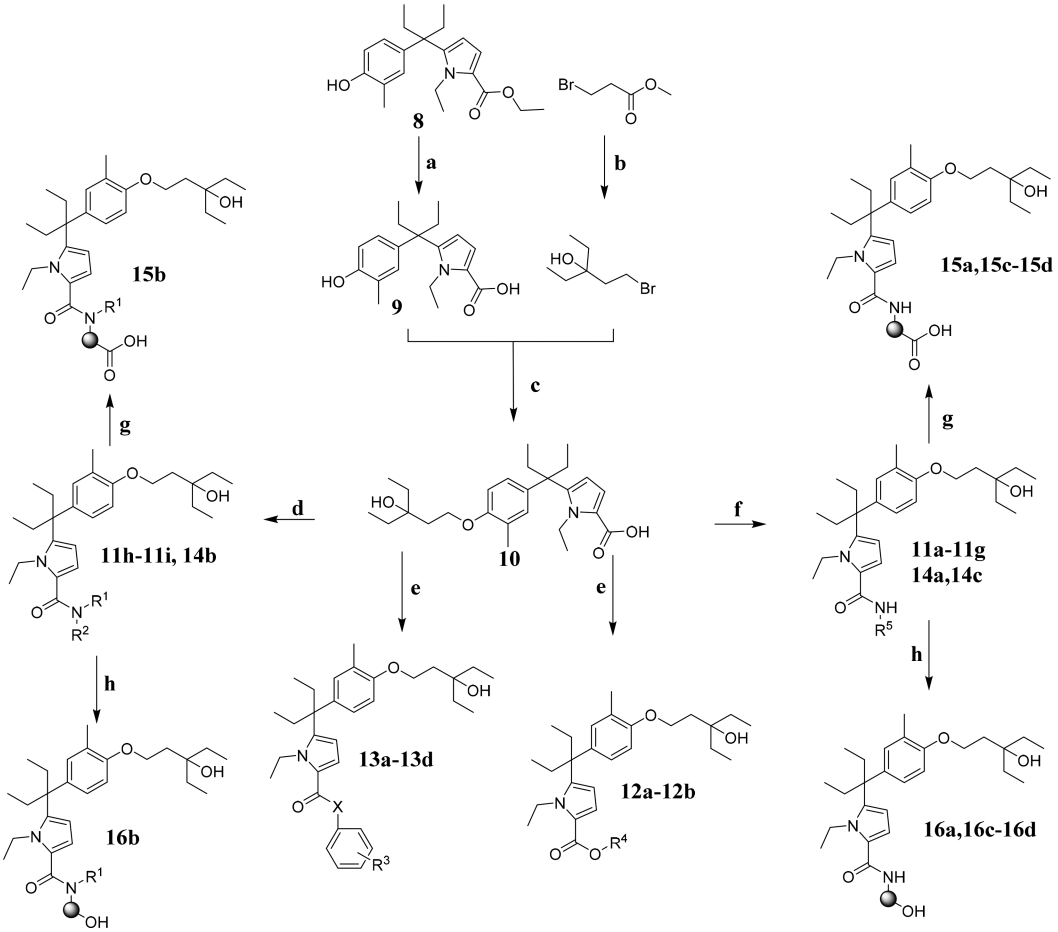

[a]Reagents and reaction conditions: (a) KOH, C_2H_5OH, 70 °C, overnight. (b) EtMgBr, Et_2O, 30 °C, 2 h. (c) NaH, DMF, rt, 2.5 h. (d) Amines or amino acid methyl ester hydrochlorides, 4-nitrobenzenesulfonyl chloride, DMAP, CH_3CN, 70 °C, overnight. (e) Aryl amines, aryl esters, or alcohols; EDCI; DMAP; $CHCl_3$; 70 °C; overnight. (f) Amino acid methyl ester hydrochlorides or amines, EDCI, HOBT, Et_3N, $CHCl_3$, 25 °C, overnight. (g) $LiOH{\cdot}H_2O$, THF, H_2O, 25 °C, overnight. (h) $NaBH_4$, CH_3OH, 25 °C, 6 h.

DOI: 10.1021/acs.jmedchem.8b00106
J. Med. Chem. 2018, 61, 3059−3075

Table 1. Cellular Anti-Proliferative Activities of the Phenyl-Pyrrolyl Pentane Derivatives

	IC_{50} (μM)[a]				
compound	MCF7	PC3	Caco2	HepG2	L02
11a	3.35 ± 1.26*	2.15 ± 0.93*	0.49 ± 0.04*	0.11 ± 0.03*	2.42 ± 1.35
11b	0.057 ± 0.018*	0.040 ± 0.006*	0.017 ± 0.001*	0.15 ± 0.05*	0.37 ± 0.17*
11c	0.43 ± 0.27*	0.87 ± 0.26*	1.14 ± 0.25*	0.24 ± 0.03*	0.99 ± 0.21
11d	0.55 ± 0.16*	3.35 ± 0.95*	1.63 ± 0.59*	0.23 ± 0.12*	2.29 ± 1.28
11e	>50	17.81 ± 4.18	>50	>50	>50
11f	0.67 ± 0.34*	2.42 ± 0.83*	1.74 ± 0.43*	1.59 ± 0.21*	2.94 ± 0.93
11g	0.26 ± 0.08*	1.57 ± 0.61*	2.72 ± 0.71*	1.76 ± 0.46*	2.86 ± 1.12
11h	>50	>50	>50	46.28 ± 14.28	37.80 ± 10.28
11i	>50	12.77 ± 3.86*	>50	>50	1.19 ± 0.36
12a	>50	14.81 ± 4.18*	>50	>50	>50
12b	>50	>50	>50	>50	>50
13a	>50	>50	>50	>50	>50
13b	>50	>50	>50	>50	>50
13c	>50	23.77 ± 7.29	>50	>50	>50
13d	>50	>50	>50	>50	>50
14a	>50	>50	>50	>50	>50
14b	3.21 ± 1.57*	7.14 ± 1.63*	30.26 ± 10.37	25.31 ± 9.36*	1.99 ± 0.26
14c	0.39 ± 0.14*	5.84 ± 1.42*	3.02 ± 0.82*	>50	4.28 ± 1.84
15a	11.27 ± 2.49	13.79 ± 2.91*	19.97 ± 5.15	2.62 ± 0.91*	9.99 ± 2.55
15b	0.079 ± 0.028*	2.25 ± 0.82*	2.74 ± 1.16*	5.71 ± 2.47*	2.15 ± 0.81
15c	10.21 ± 3.21	11.17 ± 1.28*	25.19 ± 9.36	10.71 ± 1.64*	7.59 ± 1.62
15d	19.69 ± 3.37	11.69 ± 3.19*	46.47 ± 12.57	1.74 ± 0.22*	4.04 ± 0.74
16a	29.14 ± 5.76	28.39 ± 4.25	>50	>50	>50
16b	2.87 ± 1.04*	3.09 ± 0.43*	0.074 ± 0.005*	0.51 ± 0.06*	2.05 ± 0.86
16c	31.41 ± 7.92	8.76 ± 1.72*	40.24 ± 11.68	24.81 ± 10.83*	3.04 ± 1.51
16d	12.62 ± 4.63	7.87 ± 1.45*	>50	43.07 ± 13.59*	4.84 ± 1.22
sw22	2.803 ± 0.52	17.36 ± 2.65	>50	47.55 ± 3.27*	17.38 ± 1.75
calcitriol	5.59 ± 1.72	17.25 ± 3.83	4.46 ± 0.82	>50	0.67 ± 0.05

[a]Data are presented as means ± SD (n = 3). *p < 0.05 compared with the value of calcitriol.

for the treatment of cancers, osteoporosis, and skin disorders.[20,21] However, most of these classic VDR modulators have secosteroidal structures and can lead to hypercalcemia or hypercalciuria, which impedes their application in long-term cancer therapies and the translation of basic and clinical research to therapeutic agents. It was reported that calcitriol, given at a high dose (45 μg) once a week in combination with docetaxel as a prostate-cancer treatment, was terminated in a phase III trial. Part of the reason for this were the side effects of hypercalcemia, including myocardial injuries, nervous-system damage, and renal stones, resulting in lower survival rates in the treatment group compared with in the placebo group.[22] Moreover, another clinical trial revealed that calcitriol in daily oral doses of more than 2−2.5 μg led to hypercalcemia in men with recurrent prostate cancer, which limited the ability to raise the administered dose.[23] Hence, there is an urgent clinical need for a new generation of VDR modulators that do not have the risk of increasing serum calcium for cancer chemotherapy.

As early as 1999, Boehm et al. reported the first generation of nonsteroidal vitamin D modulators that exhibited no hypercalcemic potentials in vivo. Among them, LG190119 (Figure 1A) effectively inhibited LNCaP xenograft tumor growth without increasing serum calcium levels or causing any other apparent side effects.[24] On the basis of this, various groups had reported nonsteroidal derivatives with different structures.[25,26] Nonsteroidal vitamin D mimics based on a hydrophobic core of *p*-carborane have been developed by Fujii et al.[27] Furthermore, other nonsteroidal derivatives such as bis- and tris-aromatic compounds,[28] carboxylic acid derivatives,[29] and hydroxamic acid derivatives[30] have since been reported.

Recently, a series of nonsteroidal VDR derivatives with phenyl-pyrrolyl pentane skeletons were designed and synthesized by our group. Among them, sw22 (Figure 1B) significantly inhibited the proliferation of human breast adenocarcinoma cells (MCF7 cells, IC_{50} = 320 nM).[31] On the basis of that study, the pyrrolyl side chains were modified to improve the antiproliferative activity, and the results showed that the designed compounds exhibited promising antiproliferative activities in vitro.[32]

In this study, to further improve the antiproliferative effects against cancer cells and the pharmacokinetic properties in vivo, 26 novel vitamin D analogues with phenyl-pyrrolyl pentane skeletons have been designed and synthesized, and their bioactivities have been evaluated in vitro and in vivo. First, we retained the phenyl-pyrrolyl pentane skeleton, which was able to form strong hydrophobic interactions with the hydrophobic pocket of VDR.[32] Next, we introduced diethylcarbinol as the terminal hydrophobic group in the phenyl side chain to improve the biological activities, as similar modifications were reported in both secosteroidal and nonsteroidal vitamin D analogues.[27,33,34] A previous report showed that lexicalcitol (Figure 1A), which possessed a diethylcarbinol moiety in its side chain, was at least 100-fold more effective in terms of its biological activity than calcitriol.[35] Moreover, the compound MC1301, which also had a diethylcarbinol moiety, presented improved differentiation-inducing activity (Figure 1A) compared with that of calcitriol.[35] Therefore, we tried to improve

DOI: 10.1021/acs.jmedchem.8b00106
J. Med. Chem. 2018, 61, 3059−3075

the biological activities by introducing diethylcarbinol into the benzene ring as the side chain. Then, hydrophilic groups or hydrophobic groups were added in the pyrrolyl side chain to explore the effects of different substitutions on the pyrrole ring. Finally, we investigated whether both the molecules' biological activities and metabolism were enhanced on the basis of the above design and considerations (Figure 1B). Here, we describe the synthesis and biological activities of novel nonsteroidal VDR modulators with phenyl-pyrrolyl pentane skeletons and demonstrate their promising therapeutic potentials for the treatment of breast cancer and other cancers without hypercalcemic side effects.

RESULTS

Synthesis Procedures for the Target Compounds. The synthetic route of the nonsteroidal vitamin D analogues was summarized in Scheme 1. Among these compounds, key intermediate **8** was readily prepared as previously reported by our group.[31,32] Intermediate **8** underwent potassium hydroxide (KOH) hydrolysis to give intermediate **9**, which contained a carboxyl group. The hydroxyl of **9** was directly reacted with 1-bromo-3-ethyl-pentan-3-ol to obtain key intermediate **10**. Target compounds **11a**−**11i**, **12a**, **12b**, **13a**−**13d**, and **14a**−**14c** were prepared in a single step by coupling intermediate **10** with different amines, alcohols, amino acid methyl ester hydrochlorides, aryl amines, or esters. Compounds **15a**−**15d** were synthesized through hydrolysis reactions. The amino acid or ester compounds were reduced by sodium borohydride in methanol to obtain compounds **16a**−**16d**.

Antiproliferative Effects on Cancer-Cell Lines in Vitro. The nonsteroidal vitamin D analogues with phenyl-pyrrolyl pentane skeletons were synthesized and screened for antiproliferative activities against a panel of four different cancer-cell lines: a human-breast-cancer-cell line (MCF7 cells),[36] a human-prostate-cancer-cell line (PC3 cells),[37] a human-colorectal-adenocarcinoma-cell line (Caco2 cells),[38] and a human-liver-cancer-cell line (HepG2 cells),[39] all of which expressed VDR as previously reported. We confirmed VDR-protein expression in the different cell types by Western blots and observed the relatively high expression of the VDR protein in MCF7 cells (Figure S1). As shown in Table 1, **11b** exhibited the best antiproliferative activity, with IC_{50} values of 57, 40, 17, and 150 nM for MCF7, PC3, Caco2, and HepG2 cells, respectively, and thus was more potent than both the prototype compound, sw22, and the positive-control compound, calcitriol. In addition, **11a**, **11c**, **11d**, **11f**, **11g**, **15b**, and **16b** also showed better antiproliferative activities against the four cancer-cell lines than sw22 and calcitriol. It seemed that the R^2 substitutions at the ends of the pyrrole-ring side chains of the compounds (Scheme 2) might be crucial for their anticancer activities. The compounds with hydrophilic groups, such as tertiary amines, morpholine rings, or carboxyls, at the end of pyrrole-ring side chain (**11a**, **11b**, **11d**, **11g**, and **15b**) showed more potent antiproliferative activities than did those bearing hydrophobic groups, such as trifluoromethyl, benzene, alkynyl, or ester groups (**12a**, **12b**, **13a**−**13d**, **14a**, and **14b**).

Additionally, the human normal hepatic cell line (L02 cells) was selected to evaluate the selective cytotoxicities of the designed compounds against normal cells, a surrogate experiment determining the compounds' systemic toxicity in vivo. The results revealed that **11a**, **11b**, **11d**, **11g**, and **15b** were less toxic (IC_{50} = 0.67 μM) against L02 cells compared with their lead compound, sw22, and with calcitriol. Together, these results suggested that **11a**, **11b**, **11d**, **11g**, and **15b** may possess selective antiproliferative potentials against cancer cells.

Scheme 2. Structures of the Phenyl-Pyrrolyl Pentane Series of Nonsteroidal VDR Derivatives

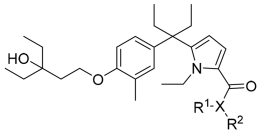

11a: X=N, R^1=H, R^2=$(CH_2)_3N(CH_3)_2$
11b: X=N, R^1=H, R^2=$(CH_2)_3N(C_2H_5)_2$
11c: X=N, R^1=H, R^2=$(CH_2)_2N(CH_3)_2$
11d: X=N, R^1=H, R^2=$(CH_2)_2N(C_2H_5)_2$
11e: X=N, R^1=H, R^2=CH_2CN
11f: X=N, R^1=H, R^2=$(CH_2)_2NH_2$
11g: X=N, R^1=H, R^2= 
11h: X=N, R^1=$(CH_2)_2CN$, R^2=$(CH_2)_2CN$
11i: X=N, R^1=CH_3, R^2=$CH_2CH{=}CH_2$
12a: X=O, R^2=$CH(CH_3)C{\equiv}CH$
12b: X=O, R^2=$(CH_2)_2C{\equiv}CH$
13a: X=O, R^2= 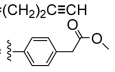
13b: X=N, R^1=H, R^2= 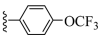
13c: X=N, R^1=H, R^2= 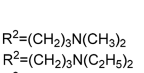
13d: X=N, R^1=H, R^2= 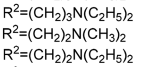
14a: X=N, R^1=H, R^2=$CH(CH(CH_3)C_2H_5)COOCH_3$
14b: X=N, R^1=CH_3, R^2=$CH_2COOC_2H_5$
14c: X=N, R^1=H, R^2=$CH(COOCH_3)CH_2COOCH_3$
15a: X=N, R^1=H, R^2=$CH(CH(CH_3)C_2H_5)COOH$
15b: X=N, R^1=CH_3, R^2=CH_2COOH
15c: X=N, R^1=H, R^2=$CH(COOCH_3)CH_2COOH$
15d: X=N, R^1=H, R^2=$CH(CH_3)COOH$
16a: X=N, R^1=H, R^2=$CH(CH(CH_3)C_2H_5)CH_2OH$
16b: X=N, R^1=CH_3, R^2=$(CH_2)_2OH$
16c: X=N, R^1=H, R^2=$CH(CH_2OH)CH_2CH_2OH$
16d: X=N, R^1=H, R^2=$CH(CH_3)CH_2OH$

Synthesized Compounds Exhibiting VDR-Modulating Activities. *In Vitro HL-60-Differentiation-Inducing Activity.* Calcitriol was known to induce HL-60-cells to differentiate into macrophages or monocytes by activating VDR signaling.[40] Recent studies used measurements of the differentiation activities of HL-60 cells treated with different vitamin D analogues to determine the compounds' VDR-agonistic activities.[41,42] First, we investigated whether our synthesized compounds were efficient inducers of HL-60-cell differentiation (Table 2).

Table 2. HL-60-Differentiation-Inducing Activities of the Synthesized Compounds

compound	EC_{50} (nM)[a]	compound	EC_{50} (nM)[a]
11a	5.000 ± 1.3*	**13d**	1630 ± 486.2
11b	11.36 ± 2.7	**14a**	>10 000
11c	82.00 ± 7.8	**14b**	520.0 ± 28.4
11d	2.300 ± 1.1*	**14c**	21.00 ± 8.2
11e	1080 ± 114.9	**15a**	860.0 ± 124.7
11f	156.0 ± 13.7	**15b**	89.00 ± 15.3
11g	238.0 ± 6.2	**15c**	26.00 ± 5.9
11h	>10 000	**15d**	66.00 ± 17.9
11i	>10 000	**16a**	450.0 ± 26.3
12a	2653 ± 83.5	**16b**	52.74 ± 11.9
12b	6033 ± 491.3	**16c**	2494 ± 563.2
13a	>10 000	**16d**	96.00 ± 7.3
13b	>10 000	sw22	8.500 ± 1.2
13c	5900 ± 1629.2	calcitriol	9.000 ± 1.2

[a]The VDR-agonistic activity was measured as the HL-60-differentiation-inducing affinity. Data are presented as means ± SD (n = 3). *p < 0.05 compared with the value of calcitriol.

Consistent with their potent effects on cancer-cell viability, compounds **11a**−**11d**, **11f**, **11g**, **15b**, and **16b** showed excellent differentiation-inducing activities, with EC_{50} values in the nanomolar range (EC_{50} = 2.3−238 nM) when the pyrrolyl side chain contained a hydrophilic group (a tertiary amine, primary amine, morpholine ring, carboxyl, or hydroxyl), suggesting that these compounds may possess VDR-agonistic

DOI: 10.1021/acs.jmedchem.8b00106
J. Med. Chem. 2018, 61, 3059−3075

activities. In contrast, compounds **11e**, **11h**, and **11i**, which had no hydrophilic groups in their side chains, induced HL-60 differentiation with EC_{50} values in the micromolar range, indicating that having a hydrophilic group in the side chain of the pyrrole ring might be important for VDR-agonistic activities.

Transactivation and Transcription Activity. The VDR-transactivation activities of the three compounds **11b**, **11g**, and **15b** were evaluated by a luciferase-reporter assay in a human-kidney-cell line (HEK293 cells) in order to further prove their VDR modulating activities. The three compounds showed concentration-dependent transactivation activities and significant partial-agonistic activities compared with the DMSO control. Among them, **15b** appeared to be the most potent compound, whereas compounds **11b** and **11g** had activities similar to that of the natural hormone calcitriol (Figure 2).

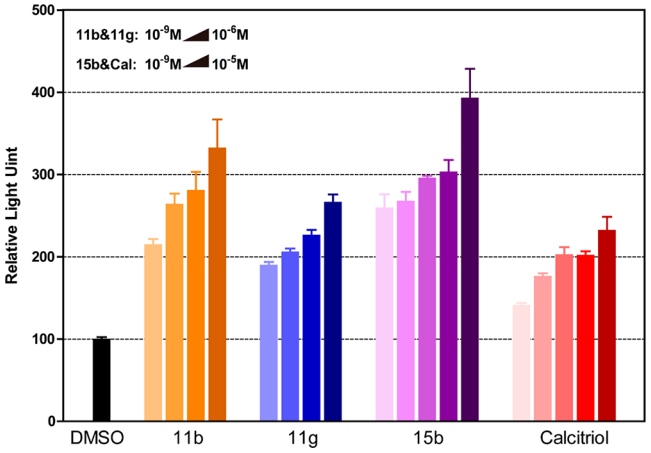

Figure 2. Transcriptional activities of compounds **11b**, **11g**, and **15b** compared with that of calcitriol in HEK293 cells. HEK293 cells were cotransfected with the pGL4.27-SPP×3-Luci reporter plasmid, pCMV-VDR, and pCMV-hRXR*α*. The cells were treated with several concentrations of **11b**, **11g**, **15b**, and calcitriol. After 24 h, the cells were harvested to test their luciferase activities.

Furthermore, **11b** and **11g** activated the expression of the endogenous *CYP24a1* gene strongly in MCF7 cells (Figure S2), suggesting that **11b** and **11g** might be novel VDR modulators for further investigation.

VDR-Binding Affinity. Because these vitamin D analogues with phenyl-pyrrolyl pentane skeletons (**11b**, **11d**, **11g**, and **15b**) were potent in terms of affecting cancer-cell viability (Table 1), HL-60-cell differentiation (Table 2), and VDR-signaling activation (Figure 2), we further examined whether these analogues could bind directly to the VDR protein in vitro with a ligand-binding assay. Compounds **11e** and **13d**, with little differentiation-inducing activities or antiproliferative activities in cancer cells showed lower potencies (IC_{50} > 500 nM) than sw22 and calcitriol under equilibrium conditions in vitro, whereas the analogues (**11b**, **11d**, and **11g**) that were more potent in the cell-based assays (HL-60 differentiation in Table 2 and VDR transactivation in Figure 2) did demonstrate binding to the VDR protein, and **11b** and **11d** had the best binding abilities (Figure 3). We hypothesized that the lower VDR-binding affinities of the phenyl-pyrrolyl pentane derivatives might be the result of having fewer hydrogen bonds, the most important bonds for interactions between the ligand and

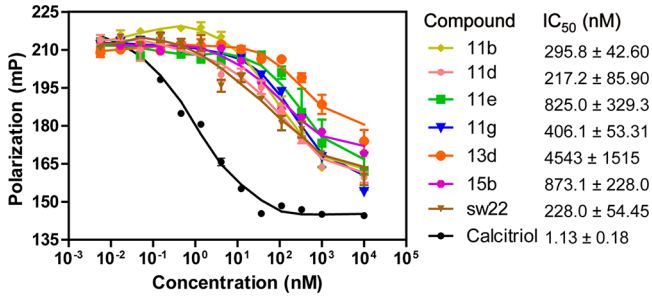

Figure 3. VDR-binding abilities of the compounds measured by fluorescence-polarization assays. Fluorescence-polarization-competition assay were performed under equilibrium conditions in vitro. The competence of the Fluormone VDR Red ligand from the VDR-LBD with the different compounds are shown (n = 3).

the ligand-binding domain of VDR (VDR-LBD), than the natural hormone calcitriol.

Molecular-Docking Study. A docking study was performed to investigate the VDR-binding characteristics of the phenyl-pyrrolyl pentane derivatives. As the vitamin D analogues (**11b**, **11d**, and **11g**) possessed a flexible side chain in the benzene ring, we first investigated the feasibility of our docking model by predicting the structure complexes between such flexible analogues and the VDR-LBD. LG190178 is a representative nonsteroidal vitamin D analogue possessing a similar flexible 2-hydroxy-3,3-dimethylbutoxy phenyl side chain (Figure S3A,B) that sits in the ligand-binding pocket in the same position as calcitriol in the VDR-LBD−calcitriol complex.[26,43,44] Therefore, we determined whether the in silico docking structure of VDR-LBD−LG190178 could reproduce the X-ray crystal structure of the VDR-LBD−LG190178 complex (PDB ID: 2ZFX).[43] The docking results showed that the in silico docking structure of the VDR-LBD−LG190178 complex could be superimposed on the X-ray crystal structure of VDR-LBD−LG190178 (Figure S3C) with a root-mean-squared deviation equaling 0.5031, which suggested that the docking model was repeatable and reliable for predicting the structure complex between the VDR-LBD and the flexible nonsteroidal vitamin D analogues.

Then, binding models of **11g** and **15b** with VDR-LBD (PDB ID: 2ZFX) were predicted, and the most suitable conformations of the ligands were selected on the basis of the calculated docking scores by means of the bonding strengths (Figure 4). The results showed that **11g** could form hydrogen bonds with VDR-LBD (the hydroxyl group at the terminus of the phenyl side chain formed hydrogen bonds with His301 and His393, and the O of the morpholine ring of the pyrrolyl side chain formed hydrogen bonds with Asp144 and Tyr232). Additionally, the hydroxyl group at the terminus of the phenyl side chain of **15b** formed the same hydrogen bond with His393 and His301, and the terminal carboxyl group of the pyrrolyl side chain formed a weak hydrogen bond with Arg270. Moreover, **11g** and **15b** also had intense van der Waals interactions between VDR-LBD and their phenyl-pyrrolyl pentane skeletons that were similar to those of calcitriol.[45]

It was reported that calcitriol could form hydrogen bonds with VDR-LBD (the 25-OH group could form hydrogen bonds with His301 and His393, the 1-OH group could form hydrogen bonds with Ser233 and Arg270, and the 3-OH group could form hydrogen bonds with Tyr139 and Ser274).[44] The hydrogen bonds formed by the hydroxyl groups at the termini of phenyl side chains of **11g** and **15b** interacting with His393

DOI: 10.1021/acs.jmedchem.8b00106
J. Med. Chem. 2018, 61, 3059−3075

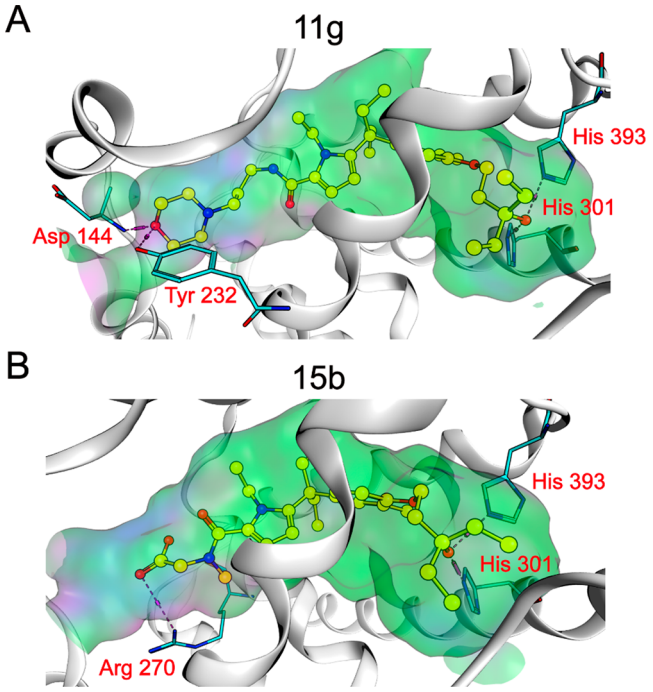

Figure 4. Predicted-binding models of **11g** (A) and **15b** (B). The VDR-LBD of PDB reference 2ZFX was used in the molecular-docking analysis performed with Glide 5.5 in Schrödinger 2009. The most suitable conformations of the ligands were selected on the basis of the docking scores calculated by means of the bonding strengths. The hydroxyl group at the end of phenyl-ring side chain of compound **11g** (A) was able to form hydrogen bonds with the His393 and His301 of the VDR-LBD. On the other side of the structure, the O of the morpholine ring bonded with Asp144 and Try232. The hydroxyl group beside phenyl of compound **15b** (B) was able to form hydrogen bonds with His393 and His301, and the terminal carboxyl group formed a hydrogen bond with Arg270.

and His301 were the same as those of calcitriol. It was interesting that the pyrrolyl side chain of **11g** formed hydrogen bonds with Asp144 and Tyr232 but not with Ser233 or Arg270 on the other side, which resulted from the spatial-configuration-reversal structure of the morpholine ring. However, the 3-OH group of calcitriol also bonded with Tyr139 and Ser274 to form additional hydrogen bonds that **11g** and **15b** did not have, suggesting that **11g** and **15b** had lower binding affinities with VDR-LBD than calcitriol.[44]

Inhibition of MCF7 Cell Growth by 11b, 11d, and 11g via Induction of Cell-Cycle Arrest and Apoptosis. As compounds **11b**, **11d**, **11g**, and **15b** showed the most potent VDR bindings, transactivations, and cancer-cell-antiproliferative activities, they were selected for further biological-activity evaluations.

Previous studies showed that vitamin D analogues such as calcitriol could prevent tumor progression by inhibiting cell proliferation and inducing apoptosis.[1,4,39,46] To explore the underlying mechanism for the reduced viabilities of the MCF7 cells, we investigated the effects of **11b**, **11d**, **11g**, and **15b** on the cell cycle by flow cytometry. Treatment of MCF7 cells with **11b**, **11d**, and **11g** effectively arrested the cells in the G0/G1 phase of the cell cycle. The populations of cells in the G0/G1 phase dramatically increased compared with that in the calcitriol-treated group (Figure 5A,B). The effect of cell-cycle arrest was also observed in HepG2 cells after they were treated with compounds **11b**, **11g**, and **15b** (Table S1). Then, we investigated whether **11b**, **11d**, **11g**, and **15b** might induce apoptosis in MCF7 cells. MCF7 cells were treated with each compound at concentrations of 1 μM for 24 h. The percentages of apoptotic MCF7 cells were measured by staining with annexin V−FITC and propidium iodide (PI). After that, we analyzed the DNA contents of the cells by flow cytometry, as described in the Experimental Section. We discovered that **11b**, **11d**, **11g**, and **15b** could promote the apoptosis of MCF7 cells compared with DMSO in the control group. Moreover, the proportion of early apoptotic cells (annexin V−FITC positive and propidium iodide negative) significantly increased in the **11d**-, **11g**-, and **15b**-treatment groups compared with in the calcitriol-treatment group (Figure 5C,D).

Previous studies reported that MART-10, a new analogue of calcitriol, could up-regulate the protein levels of p21 and p27, arrest cancer cells at the G_0/G_1 phase, and promote cell apoptosis. Moreover, other studies also determined that VDR modulators could cause cell apoptosis and the accumulation of cells in the G_0/G_1 phase, which was associated with the up-regulation of p21- and p27-protein levels in cells.[39,46−48] Hence, we speculated that our derivatives could arrest the tumor cells in the G_0/G_1 phase through the up-regulation of p21 and p27. After the MCF7 cells were treated with **11b** or **11g** at a concentration of 1 μM for 24 h, the expression levels of p21 and p27 were examined. Western-blot assays showed that treatment with **11b** and **11g** increased p21- and p27-expression levels in MCF7 cells (Figure S5). A real-time-quantitative-PCR assay revealed that **11b** and **11g** also increased the mRNA levels of p21 and p27 (Figure S4). Furthermore, the relative expression levels of Bax and Bak mRNA were elevated in MCF7 cells 24 h after the treatments with the different compounds. The results revealed that treatment with **11b** and **11g** dramatically increased the expression levels of the pro-apoptotic Bax and Bak in MCF7 cells (Figure S4). Taken together, the results demonstrated that **11b**, **11d**, and **11g** inhibited the growth of MCF7 cells by inducing cell-cycle arrest and cell apoptosis.

Cellular Uptake and Metabolic Stabilities of 11b, 11d, and 11g. To provide more basic information on their druglike properties, the cellular uptake and metabolic stabilities of **11b**, **11d**, and **11g** in MCF7 cells were further investigated. MCF7 cells were cultured with 1 μM **11b**, **11d**, **11g**, sw22, LG190119, or calcitriol in the presence of 10% FBS for 10 or 30 min. The concentrations of these compounds in both the culture media and in the cells were determined by HPLC. The cellular uptake of **11g** was 37.9 and 38.2% at 10 and 30 min, respectively, whereas that of calcitriol was 6.5 and 10.4% at 10 and 30 min, respectively. Thus, compound **11g** was shown to be 4−5 times more effectively incorporated into MCF7 cells than calcitriol, and 2−3 times more effectively incorporated than sw22 and LG190119. In addition, more effective uptake of **11b** and **11d** were also observed to be taken up more effectively by MCF7 cells than calcitriol (Figure 6A).

When MCF7 cells were cultured up to 24 h, 27% of the calcitriol was metabolically consumed, whereas only 6% of **11g** was consumed, indicating that compound **11g** was 4 times more stable than calcitriol in MCF7 cells (Figure 6B). Overall, the results suggested that **11b**, **11d**, and **11g** possessed comparable uptake activities and metabolic stabilities to those of calcitriol.

In Vivo Calcemic-Activity Assay. An in vivo calcemic-activity assay was performed to evaluate the hypercalcemia potentials of the designed nonsteroidal modulators. Com-

DOI: 10.1021/acs.jmedchem.8b00106
J. Med. Chem. 2018, 61, 3059−3075

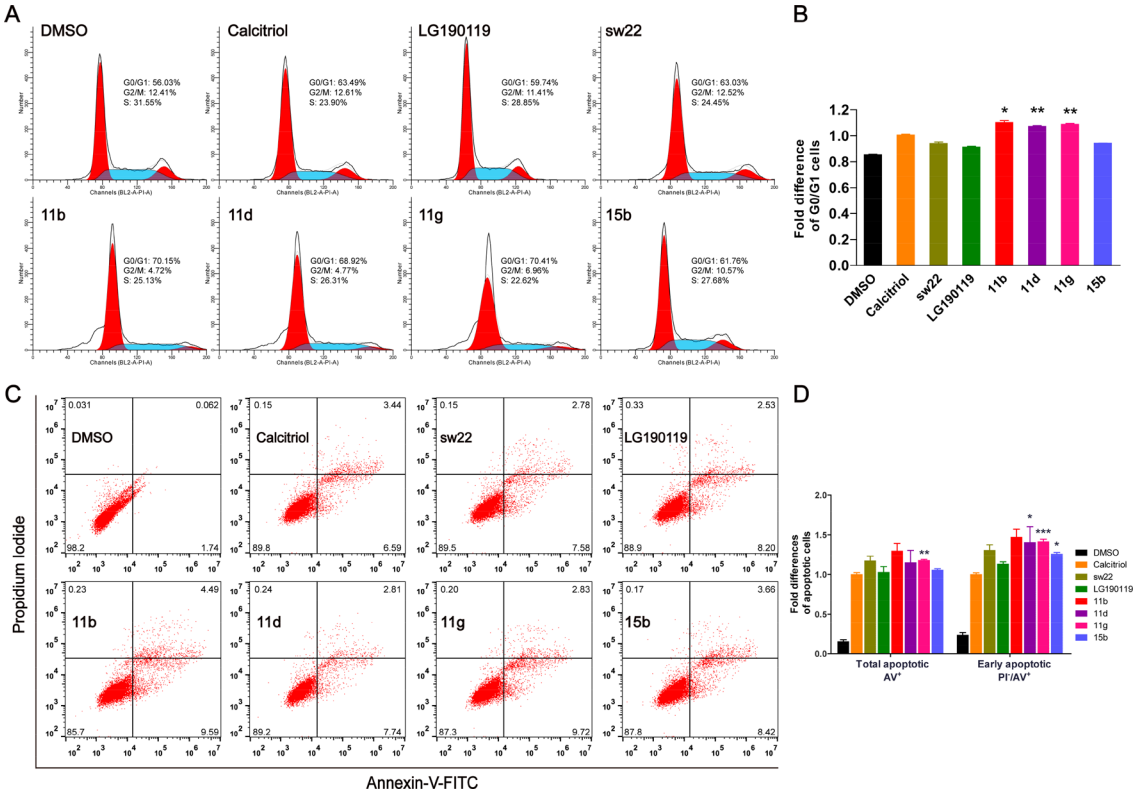

Figure 5. Cell-cycle arrest and apoptosis after treatment with vitamin D modulators in MCF7 cells. (A) Cell-cycle-phase distributions determined by flow-cytometry. The MCF7 cells were treated with each compound (1 μM) for 24 h. (B) Fold differences of the cell populations in the G0/G1 phase of the cell cycle after treatments with each compound (n = 4 for each compound). The relative differences were normalized to those of the calcitriol-treatment group. (C) Representative flow-cytometry dot plots of annexin V−FITC and PI staining for the detection of apoptotic MCF7 cells. The MCF7 cells were treated with each compound (1 μM) for 24 h. (D) Fold differences in apoptotic-cell quantifications after the cells were exposed to the compounds for 24 h (n = 3 for each compound). The relative differences were normalized to those of the calcitriol-treatment group.

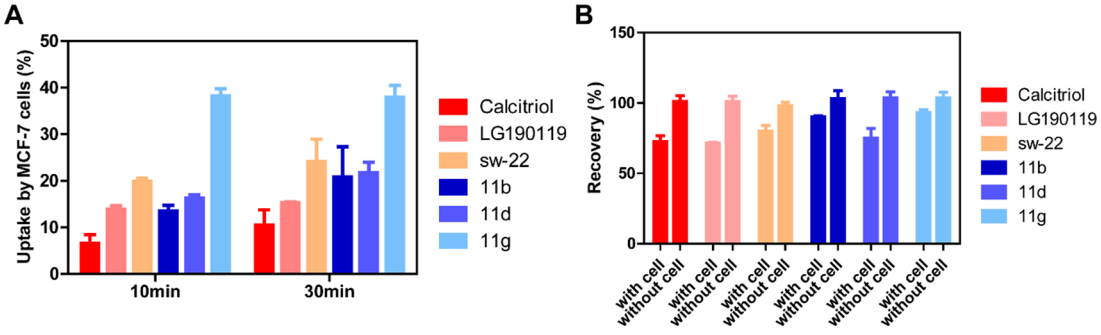

Figure 6. Uptake and metabolism stabilities of **11b**, **11d**, **11g**, calcitriol, LG190119, and sw22 in MCF7 cells. (A) MCF7 cells incubated with the different compounds (1 μM) for 10 or 30 min. The cells and media were extracted separately by chloroform/methanol (3:1, v/v). The extracts were analyzed by HPLC. (B) MCF7 cells incubated with the different compounds (1 μM) for 24 h (with cells). Similarly, each of the substrates (**11b**, **11d**, **11g**, calcitriol, LG190119, and sw22) was incubated with the medium only for 24 h (without cells). Each experimental mixture was extracted with chloroform/methanol (3:1, v/v). The extracts were analyzed by HPLC. The data were shown as the means ± SEM (n = 3).

pounds **11b**, **11d**, **11g**, and **15b** were chosen for the in vivo calcemic-activity assay; calcitriol, sw22, and LG190119 were used as the positive controls; and the vehicle was used as the negative control. The results were shown in Figure 7.

A significant increase in serum calcium was observed after the administration of calcitriol (5 μg/kg) for 7 days (11.04 mg/dL for calcitriol vs 7.05 mg/dL for saline, $p < 0.001$), whereas a dose of 0.5 μg/kg resulted in normal serum calcium levels compared with those in the vehicle group. Furthermore, **11b**, **11d**, **11g**, and **15b** at dosages of 0.5 mg/kg/day and 5 mg/kg/day had no effect on serum calcium levels. Only the intraperitoneal administration of **11d** and **11g** at dosages of 30 mg/kg/day resulted in slight elevations of serum calcium levels compared with those in the vehicle group. Therefore, the designed nonsteroidal modulators had no hypercalcemic effects in vivo.

In Vivo Antitumor-Activity Assay. To investigate the in vivo antitumor effects of **11b**, **11d**, and **11g**, a breast-tumor mouse model was established by the orthotopic transplantation of human MCF7 cells in athymic nude mice.[49] LG190119 and calcitriol were selected as the positive controls because their antitumor effects had been demonstrated in animal models or

DOI: 10.1021/acs.jmedchem.8b00106
J. Med. Chem. 2018, 61, 3059−3075

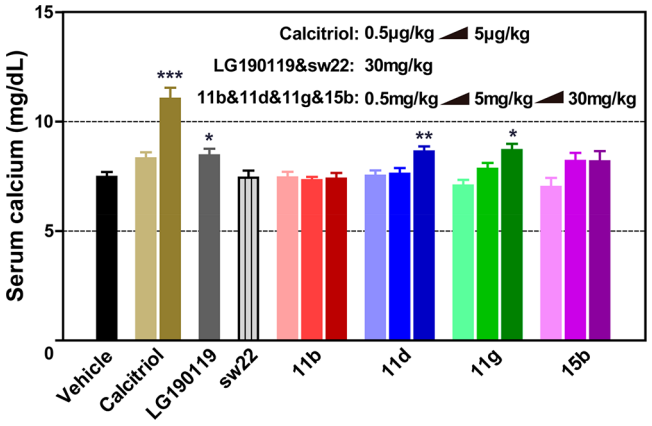

Figure 7. In vivo hypercalcemic effects of calcitriol; LG190119; sw22; and compounds **11b**, **11d**, **11g**, and **15b**. Mice were treated with **11b**, **11d**, **11g**, and **15b** in different concentrations (0.5, 5, and 30 mg/kg, ip) over a 7 day period. Calcitriol (0.5 or 5 μg/kg, ip) and LG190119 (30 mg/kg, ip), sw22 (30 mg/kg, ip) were employed as reference drugs. The data were shown as the means ± SEM (n = 6). The statistical significance (*p < 0.05, **p < 0.01, ***p < 0.001) for each concentration of serum calcium was determined via comparison with the value from the vehicle control.

human clinical trials. LG190119, the representative nonsteroidal compound,[44] was the only reported compound of the nonsteroidal analogues that displayed antitumor effects in animal cancer models. Specifically, a previous report showed that LG190119 effectively inhibited LNCaP-prostate-cancer-xenograft-tumor growth without causing hypercalcemia.[24] In addition, calcitriol has been used in a number of animal models of cancer and clinical trials for treatments for cancers such as prostate cancer and breast cancer.[1,4] The results showed that **11b**, **11d**, and **11g** significantly inhibited tumor growth compared with calcitriol (0.5 μg/kg, the concentration at which antitumor effects but no significant increases in serum calcium were observed,[49] as shown in Figure 7) and sw22 (Figure 8B,C). In addition, these three compounds also have better antitumor efficacies compared with LG190119 (10 mg/kg, the concentration at which the inhibition of prostate-tumor growth was observed).[24] Additionally, there were no significant changes in the body weights of the mice in the **11b**-, **11d**-, and **11g**-treatment groups compared to the body weights of the mice in the saline or vehicle group (Figure 8A), indicating that the three compounds had no apparent toxicity to the mice during the period of cancer treatment.

Importantly, the treatments with **11b**, **11d**, and **11g** did not increase serum calcium levels in the mice as compared to the levels in the breast-tumor-bearing mice in the control groups (Figure 8D). We further determined the proliferation and apoptosis rates of the MCF7 cells by Ki-67 immunohistochemistry and a terminal-deoxynucleotidyl-transferase dUTP-nick end-labeling (TUNEL) assay. There was a significantly low intensity of Ki-67 staining in sections of the MCF7 orthotopic tumors after they were treated with **11b** or **11g** compared with those in the calcitriol group (Figure 8E,F), which was consistent with the tumor-volume results (Figure 8B,C), suggesting that **11b** and **11g** inhibited MCF7 cell proliferation in vivo. In addition, TUNEL staining showed significantly increasing apoptosis in the breast tumors after they were treated with **11b**, **11d**, or **11g** compared with those in the sw22, LG190119, and calcitriol treatments (Figure 8G,H). Collectively, these findings suggested that **11b** and **11g** could inhibit the growth of breast cancer by suppressing proliferation and inducing apoptosis in cancer cells.

In Vivo Pharmacokinetics Study. Given their promising in vivo antitumor activities, preliminary in vivo pharmacokinetic (PK) studies of compounds **11g** and **11b** were performed in rats, and sw22 was used as the control. The results were summarized in Table 3. **11b** and **11g** displayed better pharmacokinetic properties than sw22, reaching an oral bioavailability of 36.8% and a $T_{1/2}$ value of 11.31 h after oral administration. Moreover, the $T_{1/2}$ value of **11g** after intravenous administration ($T_{1/2}$ = 4.75 h) was similar to that of calcitriol ($T_{1/2}$ = 4.27 h).[50] The results suggested that **11b** and **11g** could possess therapeutic potentials for cancer treatment.

DISCUSSION AND CONCLUSIONS

In this study, a series of novel vitamin D analogues with phenyl-pyrrolyl pentane skeletons were synthesized, and a comprehensive series of experiments were performed to validate their VDR-modulating activities and in vivo anticancer activities. This study was the first to show that **11b** and **11g**, which both had phenyl-pyrrolyl pentane skeletons, markedly inhibited MCF7-breast-tumor growth in athymic nude mice without causing increased serum calcium levels or animal weight loss, suggesting that they may be suitable for long-term cancer chemotherapies.

The compound sw22, previously reported by our group,[31] was selected as the lead compound. First, we retained the phenyl-pyrrolyl pentane skeleton to keep the VDR-binding affinity. Then, we introduced diethylcarbinol into the phenyl side chain as the terminal hydrophobic group to give **16d**. The in vitro antiproliferation results revealed that **16d** had IC_{50} ranges against different cancer cells that were similar to those of sw22 (Table 1). On the basis of this, we further explored the effects of substituting the groups on the pyrrole ring, and **11a**−**11i**, **12a**, **12b**, **13a**−**13d**, **14a**−**14c**, **15a**−**15d**, and **16a**−**16c** were thus designed and synthesized.

On the basis of the results of the in vitro antiproliferative assay and HL-60-differentiation-inducing assay, we summarized the following structure−activity relationships (SARs) of the phenyl-pyrrolyl pentane derivatives. (1) Introducing 3-ethyl-3-hydroxypentoxy into the phenyl side chain retains the antiproliferative activity against cancer cells. (2) Introducing a hydrophilic moiety, such as a hydroxy, amine, or carboxyl group, at the R^2 group (compounds **11a**−**11d**, **15a**−**15d**, and **16a**−**16d**) is important in improving the antiproliferative and HL-60-differentiation-inducing activities, whereas the introduction of a hydrophobic segment may lead to a remarkable decrease or even loss of antiproliferative and HL-60-differentiation-inducing activities, as seen with compounds **11e** and **11h**. (3) The introduction of a large group, such as benzene ring, into the R^2 group cannot be tolerated and nearly leads to a loss of antiproliferative and HL-60-differentiation-inducing activities, as seen with compounds **13a**−**13d**. (4) Introducing an alkenyl or alkynyl to the pyrroyl side chain could result in the complete disappearance of the antiproliferative and HL-60-differentiation-inducing activities, as seen with compounds **11i**, **12a**, and **12b**.

11b and **11g** showed significant VDR-agonistic activities determined by both dual-luciferase-reporter assays (Figure 2) and human-leukemia-cell-line (HL-60)-differentiation assays (Table 2), although the new analogues (**11b**, **11d**, and **11g**) showed lower competences with the Fluormone VDR Red

DOI: 10.1021/acs.jmedchem.8b00106
J. Med. Chem. 2018, 61, 3059−3075

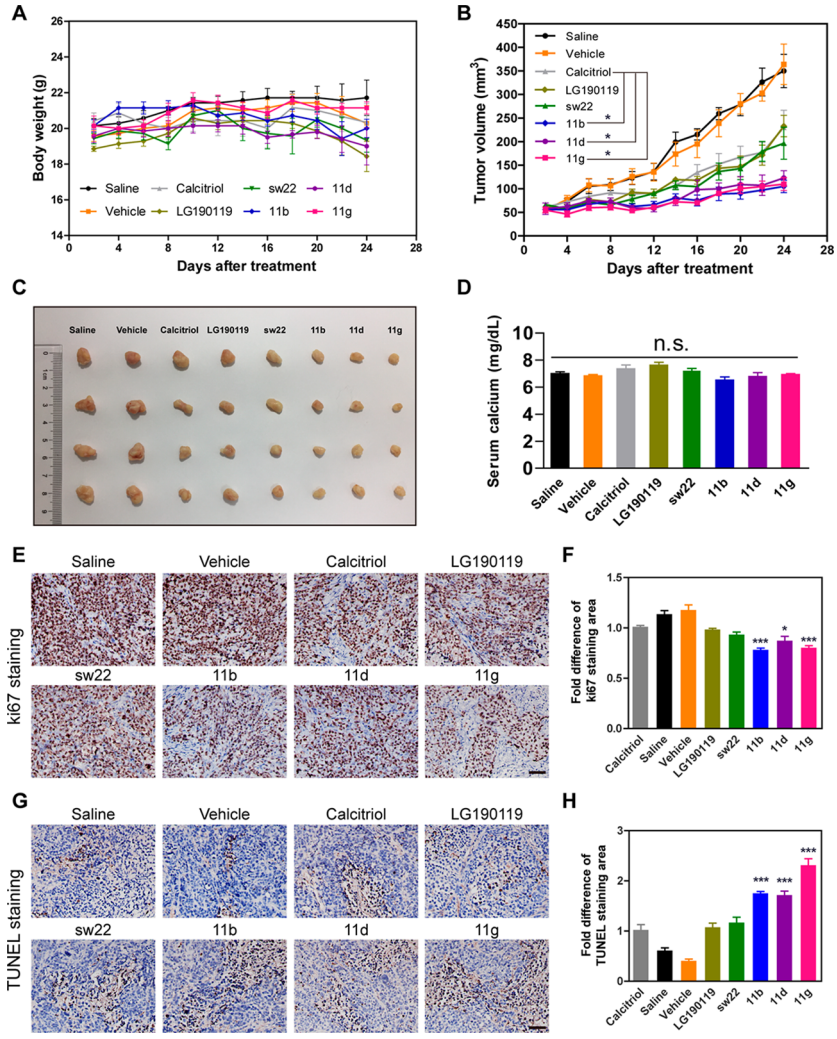

Figure 8. Antitumor effects of compounds **11b**, **11d**, and **11g** in vivo. Changes in (A) body weights and (B) tumor volumes of MCF7-bearing mice after they were treated with the vehicle (polyoxyethylenated castor oil (EL)/ethanol/saline = 1:1:18), saline, sw22 (10 mg/kg, ip), LG190119 (10 mg/kg, ip), **11b** (10 mg/kg, ip), **11d** (10 mg/kg, ip), **11g** (10 mg/kg, ip), and calcitriol (0.5 μg/kg, ip). (C) Images of excised tumors in each group. (D) Hypercalcemic effects of calcitriol, LG190119, sw22, **11b**, **11d**, and **11g** in the MCF7-tumor-bearing mice. (E) Immunohistochemistry of Ki-67 in tumor sections of MCF7-bearing mice. Scale bar, 50 μm. (F) Quantification of the percentage of the area staining positive for Ki-67 out of the total area of nuclei in each field (n = 10, 400-fold magnification). The relative differences were normalized to the values of the calcitriol-treatment group. (G) Immunohistochemistry of TUNEL in tumor sections of MCF7-bearing mice. Scale bar, 50 μm. (H) Quantification of the percentage of the area staining positive in a TUNEL assay out of the total area of nuclei in each field (n = 10, 400-fold magnification). The relative differences were normalized to the values of the calcitriol-treatment group. The statistical significances (*p < 0.05, **p < 0.01, ***p < 0.001) for **11b**, **11d**, and **11g** were determined via comparisons with the values from the vehicle control.

ligand (PolarScreen Vitamin D Receptor Competitor Assay) than calcitriol in the VDR-binding assay performed under equilibrium conditions in vitro. Therefore, the VDR-dependent cell-based assay may be more sensitive than the in vitro VDR-equilibrium-binding assay in the detection of VDR activators. We speculated that the detection of VDR binding for the less-potent nonsteroidal vitamin D analogues under equilibrium conditions in the competition binding assay with the Fluormone VDR Red ligand may be precluded by the high on-rate and low off-rate of the high-affinity Fluormone VDR Red ligand. Similar results have been reported in the VDR-binding characteristics of other nonsteroidal vitamin D analogues, including LG190119, LG190155, and LG190178.[26,29] Transcriptional activity of the VDR-downstream-target gene *Cyp24a1* can be strongly induced by calcitriol and often serves as a marker of VDR activation in the cell. In the present study, the activation of *Cyp24a1* transcription after the cells were treated with **11b** or **11g** was lower than that in the calcitriol-treatment group (Figure S2). The differences in activation levels of the *Cyp24a1* gene between the calcitriol group and the nonsteroidal-VDR-modulator groups could be due to distinctions between their metabolisms and recruitment of coactivators.[S1−S4]

Both preclinical and clinical studies support the development of vitamin D analogues as preventative and therapeutic anticancer agents,[1] however, clinically approved anticancer vitamin D drugs remain elusive. Part of the reason for the clinical failure is that high drug concentrations, which are thought to be necessary for the antitumor activities on the basis of preclinical results, are not achievable in the blood and tumors of patients because hypercalcemia intervenes.[4,55,56] One possibility for producing an effective cancer therapy is attempting to overcome the drugs' poor bioavailabilities and designing novel VDR modulators without the risk of increasing

DOI: 10.1021/acs.jmedchem.8b00106
J. Med. Chem. 2018, 61, 3059−3075

Table 3. Pharmacokinetic Profiles of Compounds 11b, 11g, and sw22 in Rats[a]

	11b			11g			sw22		
parameter	iv 5 mg/kg	ip 20 mg/kg	po 20 mg/kg	iv 5 mg/kg	ip 20 mg/kg	po 20 mg/kg	iv 5 mg/kg	ip 20 mg/kg	po 20 mg/kg
AUC (mg/L·h)	25.21 ± 3.40	30.47 ± 5.09	21.47 ± 1.26	10.37 ± 1.91	25.91 ± 2.57	15.27 ± 1.68	13.40 ± 1.07	24.76 ± 2.26	13.49 ± 1.75
$T_{1/2}$ (h)	2.97 ± 0.16	6.21 ± 1.62	6.82 ± 1.18	4.75 ± 0.85	11.73 ± 1.6	11.31 ± 2.75	2.44 ± 0.43	3.96 ± 0.53	6.89 ± 2.52
MRT (h)	3.85 ± 0.49	9.30 ± 2.32	10.97 ± 1.53	7.55 ± 0.78	17.59 ± 2.42	15.90 ± 3.18	2.82 ± 0.04	8.15 ± 0.97	10.76 ± 3.18
CL (L/h)	0.21 ± 0.032	0.68 ± 0.15	0.93 ± 0.065	0.49 ± 0.089	0.78 ± 0.082	1.31 ± 0.14	0.41 ± 0.036	0.81 ± 0.085	1.50 ± 0.21
F (%)		30.22%	21.29%		62.46%	36.80%		46.19%	25.17%

[a]Male SD rats weighing 180−220 g were used for the study (n = 4 per group). Data are presented as means ± SD.

serum calcium levels. Another would be the combination of a low-calcemic vitamin D analogue with other anticancer agents to achieve a synergistic effect on cancer therapy.[1,55] In this study, we found that **11b** and **11g** possessed good bioavailabilities and could inhibit breast-tumor growth without inducing hypercalcemia problems. This makes them promising leads for further anticancer-drug development. In addition, cancer treatments that are combinations of **11b** or **11g** with other antitumor agents (such as taxols and cisplatins) are worth further evaluation.

In summary, a series of novel phenyl-pyrrolyl pentane derivatives were synthesized as VDR modulators and analyzed for their biological activities. Among them, **11b** and **11g** were more tumor-selective in action and displayed superior therapeutic indices in vivo in the orthotopic breast-tumor model without inducing hypercalcemia, suggesting that **11b** and **11g** might be suitable for long-term treatments and chemoprevention. Overall, the structurally novel nonsteroidal tumor-selective VDR modulators with phenyl-pyrrolyl pentane skeletons provide us promising lead compounds for further anticancer-drug discovery.

EXPERIMENTAL SECTION

General Chemistry Methods. All of the commercially available chemicals and solvents were used without further purification. All of the ^{1}H NMR and ^{13}C NMR spectra were recorded on Bruker AV-300 or AV-500 instruments with $CDCl_3$ or DMSO-d_6. The chemical shifts were reported in ppm (d) with reference to the internal standard, tetramethylsilane (TMS). The signals were designated as follows: s, singlet; d, doublet; dd, doublet of doublets; t, triplet; m, multiplet. High-resolution mass spectra (HRMS) were recorded on a QSTAR XL Hybrid MS/MS mass spectrometer. The reactions were monitored by thin-layer chromatography (TLC). The compounds were separated by column chromatography on a silica gel (200−300 mesh), visualized by ultraviolet light (UV) or an iodine chamber. The purities of all of the tested compounds were >95%, as estimated by high-performance-liquid-chromatography (HPLC) analysis. The major peaks of the compounds analyzed by HPLC accounted for ≥95% of the combined total peak areas when they were monitored by a UV detector at 254 nm.

***N*-(3-(Dimethylamino)propyl)-1-ethyl-5-(3-(4-((3-ethyl-3-hydroxypentyl)oxy)-3-methylphenyl)pentan-3-yl)-1*H*-pyrrole-2-carboxamide (11a).** EDCI (0.54 g, 2.82 mmol) and HOBt (0.38 g, 2.82 mmol) were added to a solution of compound **10** (1 g, 2.32 mmol) in DMF (20 mL), and the mixture was activated by being stirred at room temperature (rt) for 0.5 h. Then, Et_3N (1.14 g, 10.21 mmol, 1.58 mL), followed by N^1,N^1-dimethylpropane-1,3-diamine (0.26 g, 2.56 mmol), was added to the mixture and reacted at rt for 4 h. Water and ethyl acetate were added and the two phases were separated. The aqueous phase was extracted with ethyl acetate and the combined organic phase was washed with water, dried over Na_2SO_4, and evaporated to get a yellow oil that was further purified to afford compound **11a** as a yellow oil (0.63 g, 55%). HRMS, ESI$^+$, m/z: calcd for $C_{31}H_{51}N_3O_3$ $(M + H)^+$ 514.4003, found 514.3998. ^{1}H NMR (300 MHz, $CDCl_3$) δ: 7.04 (1 H, d, J = 8.7 Hz), 7.01 (1 H, s), 6.74 (1 H, d, J = 8.7 Hz), 6.52 (1 H, d, J = 1.8 Hz), 6.34 (1 H, d, J = 1.8 Hz), 4.30 (2 H, q, J = 7.2 Hz), 4.13 (2 H, t, J = 6.0 Hz), 3.45 (2 H, t, J = 6.0 Hz), 3.00 (2 H, t, J = 7.2 Hz), 2.70 (6 H, s), 2.17 (3 H, s), 2.07 (2 H, m), 1.56 (4 H, m), 1.34 (3 H, t, J = 6.9 Hz), 0.90 (6 H, t, J = 7.5 Hz), 0.65 (3 H, t, J = 7.2 Hz). ^{13}C NMR (75 MHz, $CDCl_3$) δ: 162.56, 154.32, 140.17, 131.41, 130.21, 125.90, 125.05, 112.32, 109.65, 64.69, 45.82, 44.83, 43.69, 36.90, 36.33, 30.92, 30.24, 25.10, 17.26, 8.57.

***N*-(3-(Diethylamino)propyl)-1-ethyl-5-(3-(4-((3-ethyl-3-hydroxypentyl)oxy)-3-methylphenyl)pentan-3-yl)-1*H*-pyrrole-2-carboxamide (11b).** The same method as that of **11a** was used, and the starting materials were **10** and N^1,N^1-diethylpropane-1,3-diamine. Yellow oil, 0.52 g, 42% yield. HRMS, ESI$^+$, m/z: calcd for

DOI: 10.1021/acs.jmedchem.8b00106
J. Med. Chem. 2018, 61, 3059−3075

$C_{33}H_{55}N_3O_3$ $(M + H)^+$ 542.4316, found 542.4316. ^{1}H NMR (300 MHz, $CDCl_3$) δ: 7.04 (1 H, d, J = 8.4 Hz), 7.01 (1 H, s), 6.74 (1 H, d, J = 8.4 Hz), 6.51 (1 H, d, J = 1.5 Hz), 6.45 (1 H, d, J = 1.5 Hz), 4.30 (2 H, q, J = 7.2 Hz), 4.13 (3 H, t, J = 6.0 Hz), 3.46 (2 H, m), 3.02 (6 H, m), 2.21 (3 H, s), 2.08 (2 H, m), 1.07 (6 H, m), 1.55 (4 H, m), 1.34 (9 H, m), 0.90 (6 H, t, J = 7.5 Hz), 0.65 (6 H, t, J = 7.2 Hz). ^{13}C NMR (75 MHz, $CDCl_3$) δ: 162.57, 154.40, 140.19, 131.41, 130.22, 125.88, 125.02, 123.54, 112.42, 109.62, 64.70, 49.84, 46.38, 44.83, 43.66, 36.89, 30.92, 30.22, 24.29, 17.25, 8.75, 8.56.

_N_-(2-(Dimethylamino)ethyl)-1-ethyl-5-(3-(4-((3-ethyl-3-hydroxypentyl)oxy)3-methylphenyl)pentan-3-yl)-1_H_-pyrrole-2-carboxamide (11c). The same method as that of **11a** was used, and the starting materials were **10** and N^1,N^1-dimethylethane-1,2-diamine. Yellow oil, 0.59 g, 51% yield. HRMS, ESI$^+$, m/z: calcd for $C_{30}H_{49}N_3O_3$ $(M + H)^+$ 500.3847, found 500.3841. ^{1}H NMR (300 MHz, $CDCl_3$) δ: 7.04 (1 H, d, J = 8.4 Hz), 7.02 (1 H, s), 6.73 (1 H, d, J = 8.4 Hz), 6.62 (1 H, d, J = 1.5 Hz), 6.51 (1 H, d, J = 1.5 Hz), 4.29 (2 H, q, J = 7.2 Hz), 4.13 (2 H, t, J = 6.0 Hz), 3.68 (2 H, m), 3.02 (2 H, m), 2.67 (6 H, s), 2.17 (3 H, s), 1.95 (6 H, m), 1.56 (4 H, m), 1.32 (3 H, t, J = 7.2 Hz), 0.90 (6 H, t, J = 7.5 Hz), 0.65 (6 H, t, J = 7.2 Hz). ^{13}C NMR (75 MHz, $CDCl_3$) δ: 162.42, 154.37, 140.15, 131.40, 130.22, 125.92, 125.09, 123.20, 112.99, 109.65, 64.67, 58.23, 44.14, 36.09, 35.06, 30.92, 17.24, 8.59.

_N_-(3-(Diethylamino)ethyl)-1-ethyl-5-(3-(4-((3-ethyl-3-hydroxypentyl)oxy)-3-methylphenyl)pentan-3-yl)-1_H_-pyrrole-2-carboxamide (11d). The same method as that of **11a** was used, and the starting materials were **10** and N^1,N^1-dimethylethane-1,2-diamine. Yellow oil, 0.68 g, 55% yield. HRMS, ESI$^+$, m/z: calcd for $C_{32}H_{53}N_3O_3$ $(M + H)^+$ 528.4160, found 528.4152. ^{1}H NMR (300 MHz, $CDCl_3$) δ: 7.05 (1 H, d, J = 8.1 Hz), 7.02 (1 H, s), 6.73 (2 H, m), 6.47 (1 H, d, J = 1.5 Hz), 4.29 (2 H, q, J = 7.2 Hz), 4.13 (2 H, t, J = 6.0 Hz), 3.73 (2 H, m), 3.09 (6 H, m), 2.17 (3 H, s), 1.95 (6 H, m), 1.57 (4 H, m), 1.34 (9 H, m), 0.90 (6 H, t, J = 7.5 Hz), 0.66 (6 H, t, J = 7.2 Hz). ^{13}C NMR (75 MHz, $CDCl_3$) δ: 162.49, 154.37, 140.10, 131.51, 130.23, 125.87, 125.18, 123.01, 113.45, 109.64, 74.33, 64.68, 52.59, 48.05, 45.84, 44.84, 43.67, 36.90, 30.91, 17.22, 16.80, 8.59, 8.00.

1-Ethyl-5-{1-ethyl-1-[4-(3-ethyl-3-hydroxy-pentyloxy)-3-methyl-phenyl]-propyl}-1_H_-pyrrole-2-carboxylic Acid Cyanomethyl-amide (11e). The same method as that of **11a** was used, and the starting materials were **10** and amino-acetonitrile. Yellow oil, 0.96 g, 89% yield. HRMS, ESI$^+$, m/z: calcd for $C_{28}H_{41}N_3O_3$ $(M + Na)^+$ 490.3040, found 490.3031. ^{1}H NMR (300 MHz, $CDCl_3$) δ: 7.01 (1H, d, J = 8.4 Hz), 6.98 (1 H, s), 6.73 (1 H, d, J = 8.4 Hz), 6.64 (1 H, d, J = 1.5 Hz), 6.24 (1 H, d, J = 1.5 Hz), 4.32 (2 H, q, J = 7.2 Hz), 4.21 (2 H, s), 4.13 (2 H, d, J = 6.0 Hz), 2.17 (3 H, s), 1.95 (6 H, m), 1.57 (4 H, m), 1.37 (3 H, t, J = 7.2 Hz), 0.90 (6 H, t, J = 7.2 Hz), 0.65 (6 H, t, J = 7.2 Hz). ^{13}C NMR (75 MHz, $CDCl_3$) δ: 161.11, 154.54, 139.91, 131.88, 130.23, 125.88, 112.85, 109.62, 74.41, 64.68, 44.92, 43.96, 36.88, 30.25, 27.20, 17.14, 8.51, 8.01.

1-Ethyl-5-{1-ethyl-1-[4-(3-ethyl-3-hydroxy-pentyloxy)-3-methyl-phenyl]-propyl}-1_H_-pyrrole-2-carboxylic Acid (2-Amino-ethyl)-amide (11f). *Synthesis of (2-Amino-ethyl)-carbamic Acid tert-Butyl Ester (N-Boc).* Et_3N (15.17 g, 0.15 mol, 20.96 mL) was dropped into a solution of ethylenediamine in CH_3OH (150 mL), and then the reaction solution was added to a solution of di-*tert*-butyl dicarbonate (10.88 g, 49.94 mmol) in CH_3OH at rt, which was stirred for 5 h at rt. Then, an aqueous solution of 1 M NaH_2PO_4 (60 mL) and ether (60 mL) were added to the solution, and the two phases were separated. Then, the aqueous phase was adjusted to approximately pH 9 with 1 M NaOH and extracted with ethyl acetate. The combined organic phase was washed with brine, dried over Na_2SO_4, and evaporated to get a white solid (4.37 g, 55%).

{2-[(1-Ethyl-5-{1-ethyl-1-[4-(3-ethyl-3-hydroxy-pentyloxy)-3-methyl-phenyl]-propyl}-1H-pyrrole-2-carbonyl)-amino]-ethyl}-carbamic Acid tert-Butyl Ester (10-N-Boc). The same method as that of **11a** was used, and the starting materials were **10** and N-Boc. White oil, 0.13 mg, 50% yield.

1-Ethyl-5-{1-ethyl-1-[4-(3-ethyl-3-hydroxy-pentyloxy)-3-methyl-phenyl]-propyl}-1H-pyrrole-2-carboxylic Acid (2-Amino-ethyl)-amide (11f). A solution of hydrochloric acid (3 mL) was added to a solution of 10-*N*-Boc (0.13 mg, 0.23 mmol) in saturated ethyl acetate and left at 0 °C overnight. Then, the reaction solution was adjusted to approximately pH 7 with 1 M $NaHCO_3$ and extracted with ethyl acetate. The combined organic phase was washed with brine, dried over Na_2SO_4, and a white oil was obtained, which was further purified by column chromatography with dichloromethane/methanol (15:1, v/v) to afford compound **11f** as a white solid (0.094 mg, 87%). HRMS, ESI$^+$, m/z: calcd for $C_{28}H_{45}N_3O_3$ $(M + H)^+$ 472.3534, found 472.3527. ^{1}H NMR (300 MHz, $CDCl_3$) δ: 6.99 (2 H, m), 6.72 (1 H, d, J = 7.8 Hz), 6.52 (1 H, d, J = 1.5 Hz), 6.25 (1 H, d, J = 1.5 Hz), 4.29 (2 H, m), 4.11 (2 H, m), 3.44 (2 H, m), 2.96 (2 H, m), 2.15 (3 H, s), 1.95 (6 H, m), 1.56 (4 H, m), 1.31 (3 H, m), 0.89 (6 H, t, J = 7.2 Hz), 0.63 (6 H, m). ^{13}C NMR (75 MHz, $CDCl_3$) δ: 160.76, 154.47, 140.12, 131.38, 130.90, 125.93, 125.08, 125.48, 112.45, 109.67, 74.39, 68.15, 64.61, 44.80, 43.73, 39.10, 35.94, 30.93, 30.14, 29.70, 23.73, 17.22, 16.81, 8.54, 8.02.

1-Ethyl-5-{1-ethyl-1-[4-(3-ethyl-3-hydroxy-pentyloxy)-3-methyl-phenyl]-propyl}-1_H_-pyrrole-2-carboxylic Acid (3-Morpholin-4-yl-propyl)-amide (11g). The same method as that of **11a** was used, and the starting materials were **10** and 3-morpholin-4-yl-propylamine. Yellow oil, 0.14 g, 52% yield. HRMS, ESI$^+$, m/z: calcd for $C_{33}H_{53}N_3O_4$ $(M + H)^+$ 556.4109, found 556.4104. ^{1}H NMR (300 MHz, $CDCl_3$) δ: 7.02 (1 H, d, J = 8.4 Hz), 7.00 (1 H, s), 6.72 (1 H, d, J = 8.4 Hz), 6.57 (1 H, d, J = 1.8 Hz), 6.20 (1 H, d, J = 1.8 Hz), 4.32 (2 H, q, J = 6.9 Hz), 4.12 (2 H, t, J = 6.0 Hz), 3.59 (4 H, t, J = 4.2 Hz), 3.39 (2 H, m), 2.58 (6 H, m), 2.16 (3 H, s), 1.94 (6 H, m), 1.78 (2 H, m), 1.57 (4 H, m), 1.36 (3 H, t, J = 7.2 Hz), 0.90 (6 H, t, J = 7.5 Hz), 0.62 (6 H, t, J = 7.2 Hz). ^{13}C NMR (75 MHz, $CDCl_3$) δ: 162.18, 154.26, 140.24, 131.32, 130.18, 125.81, 125.07, 124.30, 111.36, 109.58, 74.32, 66.04, 64.61, 58.09, 53.44, 44.83, 43.65, 38.89, 36.90, 30.94, 24.43, 17.27, 8.49, 8.01.

1-Ethyl-5-{1-ethyl-1-[4-(3-ethyl-3-hydroxy-pentyloxy)-3-methyl-phenyl]-propyl}-1_H_-pyrrole-2-carboxylic Acid Bis(2-cyano-ethyl)-amide (11h). DMAP (0.59 g, 4.8 mmol) was added to a solution of compound **10** (0.5 g, 1.16 mmol) in CH_3CN (10 mL) at 60 °C for 30 min. The mixture was added to 4-nitrobenzenesulfonyl chloride (0.28 g, 1.3 mmol) and was heated to 70 °C for 3 h. Then, 3-(2-cyano-ethylamino)-propionitrile (0.16 g, 1.3 mmol) was dropped into the mixture, which was refluxed for 12 h. Water was added and the two phases were separated. The aqueous phase was extracted with ethyl acetate, and the combined organic phase was washed with water, dried over Na_2SO_4, and evaporated to get a yellow oil that was further purified by column chromatography with ethyl acetate/hexane (1:5, v/v) as the eluent to get a white oil (0.43 g, 68%). HRMS, ESI$^+$, m/z: calcd for $C_{32}H_{46}N_4O_3$ $(M + Na)^+$ 557.3462, found 557.3465. ^{1}H NMR (300 MHz, $CDCl_3$) δ: 7.02 (1 H, d, J = 8.4 Hz), 7.00 (1 H, s), 6.75 (1 H, d, J = 8.4 Hz), 6.60 (1 H, d, J = 1.5 Hz), 6.04 (1 H, d, J = 1.5 Hz), 4.12 (4 H, m), 3.83 (4 H, t, J = 6.6 Hz), 2.67 (4 H, t, J = 6.6 Hz), 2.18 (3 H, s), 1.95 (6 H, m), 1.56 (4 H, m), 1.37 (3 H, t, J = 7.2 Hz), 0.91 (6 H, t, J = 7.5 Hz), 0.67 (6 H, t, J = 7.2 Hz). ^{13}C NMR (75 MHz, $CDCl_3$) δ: 165.07, 154.55, 139.72, 131.51, 130.16, 125.95, 123.80, 122.25, 117.50, 112.40, 109.67, 74.34, 64.68, 45.07, 43.11, 36.91, 30.95, 17.12, 8.64, 8.01.

1-Ethyl-5-{1-ethyl-1-[4-(3-ethyl-3-hydroxy-pentyloxy)-3-methyl-phenyl]-propyl}-1_H_-pyrrole-2-carboxylic Acid Allyl-methyl-amide (11i). The same method as that of **11h** was used to prepare **11i** from **10** and allyl-methyl-amine. White oil, 0.42 g, 76% yield. HRMS, ESI$^+$, m/z: calcd for $C_{30}H_{46}N_2O_3$ $(M + H)^+$ 483.3581, found 483.3574. ^{1}H NMR (300 MHz, $CDCl_3$) δ: 7.03 (1 H, d, J = 8.1 Hz), 7.01 (1 H, s), 6.72 (1 H, d, J = 8.1 Hz), 6.50 (1 H, d, J = 1.5 Hz), 6.08 (1 H, d, J = 1.5 Hz), 5.80 (1 H, m), 5.19 (2 H, m), 4.11 (6 H, m), 3.02 (3 H, s), 2.17 (3 H, s), 1.94 (6 H, m), 1.58 (4 H, m), 1.34 (3 H, t, J = 7.2 Hz), 0.91 (6 H, t, J = 7.5 Hz), 0.65 (6 H, t, J = 7.2 Hz). ^{13}C NMR (75 MHz, $CDCl_3$) δ: 162.87, 154.38, 140.18, 133.34, 130.40, 125.97, 124.94, 122.69, 117.13, 112.68, 109.47, 74.34, 64.69, 45.06, 42.96, 36.89, 30.94, 17.25, 16.69, 8.67, 8.01.

1-Ethyl-5-{1-ethyl-1-[4-(3-ethyl-3-hydroxy-pentyloxy)-3-methyl-phenyl]-propyl}-1_H_-pyrrole-2-carboxylic Acid 1-Methyl-prop-2-ynyl Ester (12a). DMAP (11.37 mg, 0.093 mmol) was added to a solution of compound **10** (0.2 g, 0.47 mmol) in $CHCl_3$ (10 mL), and the mixture was activated by being stirred at rt for 1 h. Then, EDCI (99.11 mg, 0.52 mmol) was added at 0 °C for 1 h, and the

DOI: 10.1021/acs.jmedchem.8b00106
J. Med. Chem. 2018, 61, 3059−3075

mixture was allowed to react for 2 h at rt. After that, 3-butyn-2-ol was dropped into the mixture, which was refluxed for 12 h and cooled. Then, the solvent was evaporated to afford the crude product, which was further purified to afford compound **12a** as a yellow oil (87 mg, 35%). HRMS, ESI$^+$, *m/z*: calcd for $C_{30}H_{43}NO_4$ $(M + Na)^+$ 504.3084, found 504.3083. ^{1}H NMR (300 MHz, $CDCl_3$) δ: 7.02 (1 H, d, J = 7.8 Hz), 7.00 (1 H, s), 6.75 (1 H, s), 6.71 (1 H, d, J = 7.8 Hz), 6.57 (1 H, s), 4.28 (2 H, q, J = 7.2 Hz), 4.14 (2 H, t, J = 6.0 Hz), 3.76 (1 H, s), 2.18 (3 H, s), 1.95 (6 H, m), 1.56 (7 H, m), 1.35 (3 H, t, J = 6.9 Hz), 0.91 (6 H, t, J = 7.5 Hz), 0.65 (6 H, t, J = 7.2 Hz). ^{13}C NMR (75 MHz, $CDCl_3$) δ: 160.07, 154.47, 139.99, 131.94, 130.22, 126.53, 128.88, 117.30, 109.60, 72.56, 64.69, 59.59, 44.87, 44.03, 30.94, 21.42, 17.05, 8.55, 8.00.

1-Ethyl-5-{1-ethyl-1-[4-(3-ethyl-3-hydroxy-pentyloxy)-3-methyl-phenyl]-propyl}-1*H*-pyrrole-2-carboxylic Acid But-3-ynyl Ester (12b). The same method as that of **12a** was used, and the starting materials were **10** and 3-butyn-1-ol. Yellow oil, 98 mg, 43% yield. HRMS, ESI$^+$, *m/z*: calcd for $C_{30}H_{43}NO_4$ $(M + Na)^+$ 504.3084, found 504.3078. ^{1}H NMR (300 MHz, $CDCl_3$) δ: 7.02 (1 H, d, J = 6.6 Hz), 7.00 (1 H, s), 6.73 (1 H, d, J = 6.6 Hz), 6.69 (1 H, d, J = 2.1 Hz), 6.58 (1 H, d, J = 2.1 Hz), 4.28 (4 H, m), 4.14 (2 H, t, J = 6.0 Hz), 2.60 (2 H, m), 2.18 (3 H, s), 1.93 (7 H, m), 1.54 (4 H, m), 0.90 (6 H, t, J = 7.5 Hz), 0.65 (6 H, t, J = 7.2 Hz). ^{13}C NMR (75 MHz, $CDCl_3$) δ: 160.15, 154.47, 139.95, 131.89, 130.23, 126.87, 125.87, 125.14, 1117.87, 109.59, 80.29, 74.34, 69.84, 64.68, 61.44, 44.87, 44.01, 36.90, 30.95, 19.18, 17.07, 8.55, 8.00.

1-Ethyl-5-{1-ethyl-1-[4-(3-ethyl-3-hydroxy-pentyloxy)-3-methyl-phenyl]-propyl}-4*H*-pyrrole-2-carboxylic Acid 4-Ethoxycarbonylmethyl-phenyl Ester (13a). The same method as that of **12a** was used to prepare **13a** from **10** and (4-hydroxy-phenyl)-acetic acid methyl ester. Yellow oil, 103 mg, 37% yield. HRMS, ESI$^+$, *m/z*: calcd for $C_{35}H_{47}NO_6$ $(M + NH_4)^+$ 595.3742, found 595.3741. ^{1}H NMR (300 MHz, $CDCl_3$) δ: 7.28 (2 H, m), 7.11 (4 H, m), 6.93 (1 H, d, J = 2.4 Hz), 6.76 (1 H, d, J = 8.4 Hz), 6.68 (1 H, d, J = 2.4 Hz), 4.29 (2 H, q, J = 7.2 Hz), 4.15 (2 H, t, J = 6.0 Hz), 3.68 (3 H, s), 3.62 (2 H, s), 2.21 (3 H, s), 1.97 (6 H, m), 1.56 (4 H, m), 1.37 (3 H, t, J = 7.2 Hz), 0.91 (6 H, t, J = 7.5 Hz), 0.69 (6 H, t, J = 7.2 Hz). ^{13}C NMR (75 MHz, $CDCl_3$) δ: 172.43, 154.50, 149.81, 139.89, 132.40, 131.04, 130.19, 125.87, 125.89, 122.12, 118.82, 115.49, 109.69, 74.64, 64.73, 52.11, 44.92, 44.15, 40.64, 36.84, 30.90, 17.00, 8.57, 8.01.

1-Ethyl-5-{1-ethyl-1-[4-(3-ethyl-3-hydroxy-pentyloxy)-3-methyl-phenyl]-propyl}-4*H*-pyrrole-2-carboxylic Acid (4-Methoxy-phenyl)-amide (13b). The same method as that of **11a** was used to prepare **13b** from **10** and 4-methoxy-phenylamine. Yellow oil, 0.57 g, 46% yield. HRMS, ESI$^+$, *m/z*: calcd for $C_{33}H_{43}F_3N_2O_4$ $(M + Na)^+$ 611.3067, found 611.3072. ^{1}H NMR (300 MHz, $CDCl_3$) δ: 7.56 (2 H, m), 7.17 (2 H, m), 7.04 (1 H, d, J = 7.8 Hz), 7.02 (1 H, s), 6.77 (1 H, d, J = 7.8 Hz), 6.68 (1 H, d, J = 1.8 Hz), 6.35 (1 H, d, J = 1.8 Hz), 4.37 (2 H, q, J = 6.9 Hz), 4.15 (2 H, t, J = 6.0 Hz), 2.18 (3 H, s), 1.97 (6 H, m), 1.56 (4 H, m), 1.42 (3 H, t, J = 7.2 Hz), 0.91 (6 H, t, J = 7.5 Hz), 0.68 (6 H, t, J = 7.2 Hz). ^{13}C NMR (75 MHz, $CDCl_3$) δ: 160.35, 154.59, 139.99, 136.90, 131.72, 130.28, 126.45, 125.28, 123.75, 121.22, 117.32, 112.22, 109.61, 74.35, 64.68, 44.98, 44.03, 36.90, 30.97, 30.40, 17.23, 8.53, 8.00.

1-Ethyl-5-{1-ethyl-1-[4-(3-ethyl-3-hydroxy-pentyloxy)-3-methyl-phenyl]-propyl}-1*H*-pyrrole-2-carboxylic Acid (4-Trifluoromethyl-phenyl)-amide (13c). The same method as that of **11a** was used, and the starting materials were **10** and 4-trifluoromethyl-phenylamine. Yellow oil, 0.68 g, 51% yield. HRMS, ESI$^+$, *m/z*: calcd for $C_{33}H_{43}F_3N_2O_3$ $(M + H)^+$ 573.32, found 573.3526. ^{1}H NMR (300 MHz, $CDCl_3$) δ: 7.23 (2 H, m), 7.03 (1 H, d, J = 8.4 Hz), 7.02 (1 H, s), 6.93 (1 H, s), 6.86 (1 H, m), 6.74 (1 H, d, J = 8.4 Hz), 6.69 (1 H, d, J = 2.1 Hz), 6.58 (1 H, d, J = 2.1 Hz), 4.26 (2 H, q, J = 8.1 Hz), 4.14 (2 H, d, J = 2.1 Hz), 2.18 (3 H, s), 1.96 (6 H, m), 1.57 (4 H, m), 1.35 (3 H, t, J = 8.1 Hz), 0.91 (6 H, t, J = 7.5 Hz), 0.66 (6 H, t, J = 7.2 Hz). ^{13}C NMR (75 MHz, $CDCl_3$) δ: 154.78, 140.09, 130.24, 126.45, 125.89, 117.30, 109.58, 74.36, 64.69, 59.60, 44.87, 43.94, 36.89, 30.40, 17.08, 14.45, 8.55, 8.00.

1-Ethyl-5-{1-ethyl-1-[4-(3-ethyl-3-hydroxy-pentyloxy)-3-methyl-phenyl]-propyl}-1*H*-pyrrole-2-carboxylic Acid (4-Ethoxy-phenyl)-amide (13d). The same method as that of **11a** was used to prepare **13d** from **10** and 4-ethoxy-phenylamine. Brown solid, 1.08 g, 85% yield. HRMS, ESI$^+$, *m/z*: calcd for $C_{34}H_{48}N_2O_4$ $(M + H)^+$ 549.3687, found 549.3679. ^{1}H NMR (300 MHz, $CDCl_3$) δ: 7.40 (2 H, m), 7.05 (1 H, d, J = 8.4 Hz), 7.03 (1 H, s), 6.85 (2 H, m), 6.76 (1 H, d, J = 8.4 Hz), 6.64 (1 H, d, J = 1.8 Hz), 6.30 (1 H, d, J = 1.8 Hz), 4.36 (2 H, q, J = 6.9 Hz), 4.15 (2 H, t, J = 6.0 Hz), 4.00 (2 H, q, J = 6.9 Hz), 2.19 (3 H, s), 1.96 (6 H, m), 1.56 (4 H, m), 1.37 (3 H, t, J = 6.9 Hz), 0.88 (9 H, m), 0.67 (6 H, t, J = 7.2 Hz). ^{13}C NMR (75 MHz, $CDCl_3$) δ: 159.81, 155.47, 154.54, 140.13, 131.42, 125.95, 124.27, 121.81, 114.78, 111..65, 109.58, 74.35, 64.68, 63.68, 44.97, 43.89, 37.11, 30.28, 27.09, 17.29, 16.87, 8.56, 8.01.

2-[(1-Ethyl-5-{1-ethyl-1-[4-(3-ethyl-3-hydroxy-pentyloxy)-3-methyl-phenyl]-propyl}-1*H*-pyrrole-2-carbonyl)-amino]-3-methyl-pentanoic Acid Methyl Ester (14a). The same method as that of **11a** was used, and the starting materials were **10** and L-isoleucine methyl ester hydrochloride. White oil, 0.95 g, 74% yield. HRMS, ESI$^+$, *m/z*: calcd for $C_{33}H_{52}N_2O_5$ $(M + H)^+$ 557.3949, found 557.3939. ^{1}H NMR (300 MHz, $CDCl_3$) δ: 7.03 (1 H, d, J = 8.4 Hz), 7.02 (1 H, s), 6.75 (1 H, d, J = 8.4 Hz), 6.56 (1 H, d, J = 1.8 Hz), 6.29 (1 H, d, J = 1.8 Hz), 4.67 (1 H, m), 4.29 (2 H, q, J = 7.8 Hz), 4.15 (3 H, t, J = 6.0 Hz), 3.74 (3 H, s), 2.19 (3 H, s), 1.96 (8 H, m), 1.56 (5 H, m), 1.34 (3 H, t, J = 6.9 Hz), 0.92 (12 H, m), 0.66 (6 H, t, J = 7.2 Hz). ^{13}C NMR (75 MHz, $CDCl_3$) δ: 172.96, 161.58, 154.48, 140.12, 131.18, 130.28, 125.94, 125.04, 111.54, 109.58, 74.35, 64.68, 56.14, 52.03, 44.92, 43.74, 38.22, 25.41, 17.21, 16.84, 11.58, 8.56, 8.01.

[(1-Ethyl-5-{1-ethyl-1-[4-(3-ethyl-3-hydroxy-pentyloxy)-3-methyl-phenyl]-propyl}-1*H*-pyrrole-2-carbonyl)-methylamino]-acetic Acid Ethyl Ester (14b). The same method as that of **11h** and the starting materials were **10** and sarcosine ethyl ester hydrochloride. White oil, 0.06 g, 29% yield. HRMS, ESI$^+$, *m/z*: calcd for $C_{31}H_{48}N_2O_5$ $(M + H)^+$ 529.3636, found 529.3627. ^{1}H NMR (300 MHz, $CDCl_3$) δ: 7.04 (1 H, d, J = 8.4 Hz), 7.01 (1 H, s), 6.72 (1 H, d, J = 8.4 Hz), 6.52 (1 H, d, J = 1.5 Hz), 6.07 (1 H, d, J = 1.5 Hz), 4.15 (8 H, m), 3.15 (3 H, s), 2.17 (3 H, s), 1.94 (6 H, m), 1.62 (4 H, m), 1.34 (3 H, t, J = 7.2 Hz), 1.25 (3 H, t, J = 6.9 Hz), 0.91 (6 H, t, J = 7.5 Hz), 0.65 (6 H, t, J = 7.5 Hz). ^{13}C NMR (75 MHz, $CDCl_3$) δ: 169.40, 154.39, 140.11, 130.37, 126.00, 124.96, 123.04, 109.50, 74.34, 64.69, 61.17, 45.07, 43.07, 36.89, 30.94, 17.14, 14.14, 8.66, 8.00.

2-[(1-Ethyl-5-{1-ethyl-1-[4-(3-ethyl-3-hydroxy-pentyloxy)-3-methyl-phenyl]-propyl}-1*H*-pyrrole-2-carbonyl)-amino]-succinic Acid Dimethyl Ester (14c). The same method as that of **11a** was used to prepare **14c** from **10** and L-aspartic acid dimethyl ester hydrochloride. Yellow oil, 0.62 g, 78% yield. HRMS, ESI$^+$, *m/z*: calcd for $C_{32}H_{48}N_2O_7$ $(M + H)^+$ 573.3534, found 573.3526. ^{1}H NMR (300 MHz, $CDCl_3$) δ: 7.03 (1 H, d, J = 8.4 Hz), 7.02 (1 H, s), 6.68 (1 H, d, J = 8.4 Hz), 6.56 (1 H, d, J = 1.8 Hz), 6.32 (1 H, d, J = 1.8 Hz), 4.95 (1 H, m), 4.29 (2 H, m), 4.15 (2 H, t, J = 6.0 Hz), 3.77 (3 H, s), 3.68 (3 H, s), 2.95 (2 H, m), 2.18 (3 H, s), 1.96 (6 H, m), 1.64 (4 H, m), 1.38 (3 H, t, J = 7.2 Hz), 0.91 (6 H, t, J = 7.5 Hz), 0.66 (6 H, t, J = 7.2 Hz). ^{13}C NMR (75 MHz, $CDCl_3$) δ6:171.66, 161.39, 154.47, 140.05, 131.43, 130.23, 125.87, 125.31, 125.13, 112.13, 109.58, 74.35, 64.68, 52.80, 52.03, 48.29, 44.86, 43.84, 36.88, 36.45, 30.92, 30.28, 17.19, 8.54, 8.02.

2-[(1-Ethyl-5-{1-ethyl-1-[4-(3-ethyl-3-hydroxy-pentyloxy)-3-methyl-phenyl]-propyl}-1*H*-pyrrole-2-carbonyl)-amino]-3-methyl-pentanoic Acid (15a). $LiOH{\cdot}2H_2O$ (150 mg, 3.55 mmol) was added to a solution of compound **14a** (0.2 g, 0.36 mmol) in THF (10 mL) and water (2 mL) at rt. Then, the mixture was stirred overnight. The reacted solution was added to water (20 mL), was adjusted to approximately pH 4 with 1 M HCl, and extracted with ethyl acetate. The combined organic phase was washed with brine and dried over Na_2SO_4. Then, the organic phase was evaporated, and the crude product was obtained, which was further purified by column chromatography using dichloromethane/methanol (40:1, v/v) to afford compound **15a** as a yellow oil (0.16 g, 83%). HRMS, ESI$^+$, *m/z*: calcd for $C_{32}H_{50}N_2O_5$ $(M + H)^+$ 543.3792, found 543.3792. ^{1}H NMR (300 MHz, $CDCl_3$) δ: 6.99 (1 H, s), 6.71 (1 H, d, J = 9.0 Hz), 6.54 (1 H, d, J = 9.0 Hz), 6.42 (1 H, s), 6.34 (1 H, s), 4.12 (5 H, m), 2.17 (3 H, s), 1.92 (6 H, m), 1.56 (6 H, m), 1.23 (3 H, t, J = 6.9 Hz), 1.05 (1 H, m), 0.85 (12 H, m), 0.62 (6 H, t, J = 7.2 Hz). ^{13}C NMR (75

DOI: 10.1021/acs.jmedchem.8b00106
J. Med. Chem. 2018, 61, 3059−3075

MHz, $CDCl_3$) δ: 173.15, 162.38, 154.46, 140.02, 131.16, 130.16, 126.01, 125.05, 123.79, 112.22, 109.66, 74.34, 64.63, 59.43, 44.87, 36.94, 30.91, 25.29, 17.14, 11.34, 8.57, 8.00.

[(1-Ethyl-5-{1-ethyl-1-[4-(3-ethyl-3-hydroxy-pentyloxy)-3-methyl-phenyl]-propyl}-1*H*-pyrrole-2-carbonyl)-methylamino]-acetic Acid (15b). The same method as that of **15a** was used, and the starting material was **14b**. Pink oil, 0.1 g, 77% yield. HRMS, ESI$^+$, *m*/*z*: calcd for $C_{29}H_{44}N_2O_5$ $(M + H)^+$ 501.3323, found 501.3313. ^{1}H NMR (300 MHz, $CDCl_3$) δ: 7.01 (1 H, d, *J* = 8.4 Hz), 6.99 (1 H, s), 6.72 (1 H, d, *J* = 8.4 Hz), 6.52 (1 H, d, *J* = 1.5 Hz), 6.09 (1 H, d, *J* = 1.5 Hz), 4.15 (6 H, m), 3.15 (3 H, s), 2.17 (3 H, s), 1.95 (6 H, m), 1.58 (4 H, m), 1.38 (3 H, m), 0.90 (6 H, t, *J* = 7.5 Hz), 0.65 (6 H, t, *J* = 7.2 Hz). ^{13}C NMR (75 MHz, $CDCl_3$) δ: 171.35, 165.62, 154.36, 140.02, 130.77, 125.98, 125.04, 122.32, 109.61, 74.35, 64.65, 45.04, 43.12, 36.78, 30.84, 29.70, 17.01, 8.64, 7.99.

2-[(1-Ethyl-5-{1-ethyl-1-[4-(3-ethyl-3-hydroxy-pentyloxy)-3-methyl-phenyl]-propyl}-1*H*-pyrrole-2-carbonyl)-amino]-succinic Acid 1-methyl ester (15c). The same method as that of **15a** was used to prepare **15c** from **14c**. White oil, 0.13 g, 62% yield. HRMS, ESI$^+$, *m*/*z*: calcd for $C_{31}H_{46}N_2O_7$ $(M + H)^+$ 559.3378, found 559.3366. ^{1}H NMR (300 MHz, $CDCl_3$) δ: 6.99 (1 H, d, *J* = 8.4 Hz), 6.85 (1 H, s), 6.75 (1 H, d, *J* = 8.4 Hz), 6.59 (1 H, d, *J* = 1.8 Hz), 6.33 (1 H, d, *J* = 1.8 Hz), 5.30 (1 H, m), 4.27 (2 H, m), 4.16 (2 H, t, *J* = 6.0 Hz), 3.71 (3 H, s), 3.05 (2 H, m), 2.17 (3 H, s), 1.96 (6 H, m), 1.64 (4 H, m), 1.38 (3 H, t, *J* = 7.2 Hz), 0.91 (6 H, t, *J* = 7.5 Hz), 0.66 (6 H, t, *J* = 7.2 Hz). ^{13}C NMR (75 MHz, $CDCl_3$) δ6:171.66, 161.39, 154.47, 140.05, 131.43, 130.23, 125.87, 125.31, 125.13, 112.13, 109.58, 74.35, 64.68, 52.80, 52.03, 48.29, 44.86, 43.84, 36.88, 36.45, 30.92, 30.28, 17.19, 8.54, 8.02.

2-[(1-Ethyl-5-{1-ethyl-1-[4-(3-ethyl-3-hydroxy-pentyloxy)-3-methyl-phenyl]-propyl}-1*H*-pyrrole-2-carbonyl)-amino]-propionic Acid (15d). The same method as that of **11a** was used, and the starting materials were **10** and L-alanine methyl ester hydrochloride. Intermediate **77** was obtained through the reaction. Then, the same method as that of **15a** was used to prepare **15d** from **77**. Yellow oil, 0.1 g, 71% yield. HRMS, ESI$^+$, *m*/*z*: calcd for $C_{29}H_{44}N_2O_5$ $(M + H)^+$ 501.3323, found 501.3317. ^{1}H NMR (300 MHz, $CDCl_3$) δ: 7.02 (1 H, d, *J* = 8.1 Hz), 7.00 (1 H, s), 6.74 (1 H, d, *J* = 8.1 Hz), 6.55 (1 H, d, *J* = 2.1 Hz), 6.28 (1 H, d, *J* = 2.1 Hz), 4.61 (1 H, m), 4.33 (2 H, q, *J* = 6.6 Hz), 4.16 (2 H, t, *J* = 6.0 Hz), 2.18 (3 H, s), 1.93 (6 H, m), 1.58 (4 H, m), 1.49 (3 H, d, *J* = 7.2 Hz), 1.35 (3 H, t, *J* = 6.6 Hz), 0.91 (6 H, m), 0.65 (6 H, t, *J* = 7.2 Hz). ^{13}C NMR (75 MHz, $CDCl_3$) δ: 175.38, 162.20, 154.45, 140.09, 131.57, 130.27, 125.53, 123.00, 112.48, 109.62, 74.78, 64.67, 48.32, 44.91, 43.88, 36.79, 30.25, 17.91, 17.18, 8.53, 7.99.

1-Ethyl-5-{1-ethyl-1-[4-(3-ethyl-3-hydroxy-pentyloxy)-3-methyl-phenyl]-propyl}-1*H*-pyrrole-2-carboxylic Acid (1-Hydroxymethyl-2-methyl-butyl)-amide (16a). $NaBH_4$ (0.14 g, 3.8 mmol) was added to a solution of compound **14a** (0.21 g, 0.38 mmol) in CH_3OH (10 mL) at rt, and the mixture was stirred for 0.5 h. Water was added, and the two phases were separated. Then, the aqueous phase was extracted with ethyl acetate, and the combined organic phase was dried over Na_2SO_4 and evaporated to get a white oil that was further purified by column chromatography using ethyl acetate/hexane (1:1, v/v) as the eluent to get a white solid (0.18 g, 89%). HRMS, ESI$^+$, *m*/*z*: calcd for $C_{32}H_{52}N_2O_4$ $(M + H)^+$ 529.4000, found 529.3998. ^{1}H NMR (300 MHz, $CDCl_3$) δ: 7.03 (1 H, d, *J* = 8.4 Hz), 7.02 (1 H, s), 6.75 (1 H, d, *J* = 8.4 Hz), 6.56 (1 H, d, *J* = 1.8 Hz), 6.29 (1 H, d, *J* = 1.8 Hz), 4.67 (1 H, m), 4.29 (2 H, q, *J* = 7.8 Hz), 4.15 (3 H, t, *J* = 6.0 Hz), 3.73 (2 H, m), 2.19 (3 H, s), 1.96 (8 H, m), 1.56 (5 H, m), 1.34 (3 H, t, *J* = 6.9 Hz), 0.92 (12 H, m), 0.66 (6 H, t, *J* = 7.2 Hz). ^{13}C NMR (75 MHz, $CDCl_3$) δ: 172.96, 161.58, 154.48, 140.12, 131.18, 130.28, 125.94, 125.04, 111.54, 109.58, 74.35, 64.68, 56.14, 52.03, 44.92, 43.74, 38.22, 36.89, 30.93, 25.41, 17.21, 16.84, 11.58, 8.56, 8.01.

1-Ethyl-5-{1-ethyl-1-[4-(3-ethyl-3-hydroxy-pentyloxy)-3-methyl-phenyl]-propyl}-1*H*-pyrrole-2-carboxylic Acid (2-Hydroxy-ethyl)-methyl-amide (16b). The same method as that of **16a** was used to prepare **16b** from **14b**. Yellow oil, 0.09 g, 60% yield. HRMS, ESI$^+$, *m*/*z*: calcd for $C_{29}H_{46}N_2O_4$ $(M + H)^+$ 487.3530, found 487.3521. ^{1}H NMR (300 MHz, $CDCl_3$) δ: 7.02 (1 H, d, *J* = 8.4 Hz), 7.01 (1 H, s), 6.72 (1 H, d, *J* = 8.4 Hz), 6.55 (1 H, d, *J* = 1.5 Hz), 6.11 (1 H, d, *J* = 1.5 Hz), 4.13 (4 H, m), 3.81 (2 H, t, *J* = 4.8 Hz), 3.62 (2 H, t, *J* = 4.8 Hz), 3.16 (3 H, s), 2.17 (3 H, s), 1.95 (6 H, m), 1.58 (4 H, m), 1.34 (3 H, t, *J* = 7.2 Hz), 0.91 (6 H, t, *J* = 7.5 Hz), 0.66 (6 H, t, *J* = 7.5 Hz). ^{13}C NMR (75 MHz, $CDCl_3$) δ: 166.41, 154.42, 140.08, 130.54, 128.84, 125.99, 124.99, 123.34, 113.89, 109.49, 74.36, 64.66, 61.17, 51.69, 45.07, 43.11, 36.88, 30.78, 17.17, 16.81, 8.65, 8.01.

1-Ethyl-5-{1-ethyl-1-[4-(3-ethyl-3-hydroxy-pentyloxy)-3-methyl-phenyl]-propyl}-1*H*-pyrrole-2-carboxylic Acid (3-Hydroxy-1-hydroxymethyl-propyl)-amide (16c). The same method as that of **16a** was used, and the starting material was **14c**. White oil, 0.07 g, 54% yield. HRMS, ESI$^+$, *m*/*z*: calcd for $C_{30}H_{48}N_2O_5$ $(M + H)^+$ 517.3636, found 517.3624. ^{1}H NMR (300 MHz, $CDCl_3$) δ: 7.02 (1 H, d, *J* = 8.1 Hz), 7.00 (1 H, s), 6.73 (1 H, d, *J* = 8.1 Hz), 6.59 (1 H, d, *J* = 1.5 Hz), 6.26 (1 H, d, *J* = 1.5 Hz), 4.32 (2 H, m), 4.20 (1 H, m), 4.13 (2 H, t, *J* = 6.0 Hz), 3.73 (4 H, m), 2.17 (3 H, s), 1.95 (6 H, m), 1.58 (4 H, m), 1.35 (3 H, t, *J* = 7.2 Hz), 0.90 (6 H, t, *J* = 7.5 Hz), 0.64 (6 H, t, *J* = 7.2 Hz). ^{13}C NMR (75 MHz, $CDCl_3$) δ: 163.13, 154.44, 140.15, 131.42, 130.24, 125.94, 125.21, 125.42, 111.95, 109.61, 74.49, 65.39, 64.66, 58.74, 48.17, 44.88, 43.88, 36.85, 34.56, 30.91, 30.19, 17.24, 8.53, 8.01.

1-Ethyl-5-{1-ethyl-1-[4-(3-ethyl-3-hydroxy-pentyloxy)-3-methyl-phenyl]-propyl}-1*H*-pyrrole-2-carboxylic Acid (2-Hydroxy-1-methyl-ethyl)-amide (16d). The same method as that of **16a** was used to prepare **16d** from **77**. Yellow oil, 0.4 g, 67% yield. HRMS, ESI$^+$, *m*/*z*: calcd for $C_{29}H_{46}N_2O_4$ $(M + H)^+$ 487.3530, found 487.3525. ^{1}H NMR (300 MHz, $CDCl_3$) δ: 7.02 (1 H, d, *J* = 8.4 Hz), 7.00 (1 H, s), 6.74 (1 H, d, *J* = 8.4 Hz), 6.59 (1 H, d, *J* = 1.5 Hz), 6.19 (1 H, d, *J* = 1.5 Hz), 4.31 (2 H, q, *J* = 6.9 Hz), 4.14 (2 H, t, *J* = 6.0 Hz), 3.74 (1 H, m), 3.63 (2 H, m), 2.18 (3 H, s), 1.95 (6 H, m), 1.57 (4 H, m), 1.39 (3 H, t, *J* = 6.9 Hz), 1.21 (3 H, d, *J* = 6.9 Hz), 0.91 (6 H, t, *J* = 7.5 Hz), 0.67 (6 H, t, *J* = 7.2 Hz). ^{13}C NMR (75 MHz, $CDCl_3$) δ: 162.83, 154.48, 140.18, 5.93, 131.28, 130.27, 123.78, 111.58, 109.54, 74.38, 67.82, 64.66, 47.84, 44.90, 43.80, 36.88, 30.93, 17.23, 8.54, 8.01.

Cell Lines and Cell Cultures. The cell lines (HL-60, HepG2, MCF7, PC3, Caco2, and L02) were purchased from ATCC. The HL-60 cells, HepG2 cells, and L02 cells were cultured in RPMI-1640 medium containing 10% fetal bovine serum (FBS), 100 U/mL penicillin, and 0.1 mg/mL streptomycin. MCF7 cells and PC3 cells were cultured in Dulbecco's Modified Eagle's Medium (DMEM, HyClone) containing 10% FBS, 100 U/mL penicillin (HyClone), and 0.1 mg/mL streptomycin (HyClone). Caco2 cells were cultured in DMEM containing 10% FBS, 1% nonessential amino acids (NEAA), 100 U/mL penicillin, and 0.1 mg/mL streptomycin. The cells were kept at 37 °C in a humidified atmosphere containing 5% CO_2.

Measurement of Cell-Proliferation Inhibition by an MTT Assay. Cell suspensions (200 μL, 1 × 10^5 cells/mL) were added to the wells of 96-well culture plates and incubated at 37 °C in a humidified atmosphere of 5% CO_2 for 24 h. Then, the culture medium was discarded, and the cells were treated with different concentrations of each compound dissolved in 200 μL of serum-free medium and incubated at 37 °C for 48 h. After that, 20 μL of methylthiazolyldiphenyl-tetrazolium bromide (MTT) was added to each well and incubated for an additional 4 h. The medium was replaced with 150 mL of DMSO to solubilize the purple formazan crystals, and the absorbances were measured on a microplate reader at 570 nm. The inhibition of cell growth was evaluated as the ratio of the absorbance of the sample to that of the control. Finally, the IC_{50} value of each compound was calculated using GraphPad Prism 5.0 (GraphPad Inc.).

Measurement of VDR Activation by Leukemic-Cell Differentiation. HL-60 cells (1 × 10^4 cells/mL) were plated in 96-well plates and were incubated at 37 °C in a humidified atmosphere of 5% CO_2 for 24 h. Then, the ligands were dissolved in DMSO, diluted to different concentrations with the RPMI-1640 medium (the final concentration of DMSO was 0.1%), and incubated with HL-60 cells for 96 h. After the incubation, the cells were harvested for the determination of the differentiation levels.

Nitroblue tetrazolium (NBT) and 12-*O*-tetradecanoylphorbol-13-acetate (TPA) were added to the cells to final concentrations of 0.1%

DOI: 10.1021/acs.jmedchem.8b00106
J. Med. Chem. 2018, 61, 3059−3075

NBT and 100 ng/mL TPA. The mixture was incubated at 37 °C for another 3 h, during which time the NBT was being bioreduced and turned blue-black by the differentiated cells. The differentiated cells were counted, and the percentage of differentiated cells was determined. Finally, the EC_{50} value of each ligand was calculated using GraphPad Prism 5.0.

Transfection and Transactivation Assays. Human kidney HEK293 cells were cultured in DMEM supplemented with 10% FBS, 100 U/mL penicillin, and 0.1 mg/mL streptomycin at 37 °C in a humidified atmosphere of 5% CO_2 in air. Transfections of 100 ng of the pGL4.27-SPP×3-Luci reporter plasmid containing three copies of the mouse osteopontin vitamin D response element (VDRE, 5′-GGTTCAcgaGGTTCA-3′), 20 ng of pRL-TK (Promega), 30 ng of pENTER-CMV-hVDR, and 30 ng of pENTER-CMV-hRXRα were performed in each well of a 48-well plate using an ExFect Transfection Reagent Kit (Vazyme) according to the manufacturer's protocol. After a 12 h incubation, the cells were treated with either a ligand or the DMSO vehicle and cultured for 24 h. The cells in each well were harvested with a cell-lysis buffer, and their luciferase activities were measured with a dual-luciferase-assay kit (Promega). Transactivation measured by the luciferase activity was normalized with internal Renilla luciferase expression.

VDR-Binding Characteristics of the Phenyl-Pyrrolyl Pentane Derivatives. Full-length human VDR, Fluormone VDR Red, and VDR Red Screening Buffer were purchased from Invitrogen (PolarScreen Vitamin D Receptor Competitor Assay). The assays were performed in 384-well black polypropylene plates. The test compounds and calcitriol were dissolved in DMSO and diluted with VDR Red Screening Buffer with 1% DMSO to different concentrations. The receptor−tracer complex was added to the ligands in various concentrations or to the DMSO solvent control to final concentrations of 0.7 nM VDR and 1 nM Fluormone VDR Red. Each mixture was incubated for 4 h at room temperature. Then, the fluorescence polarization was measured on an Ultra384 microplate reader (Tecan) using a 535 nm excitation filter (25 nm bandwidth) and 590 nm emission filter (20 nm bandwidth). Finally, the IC_{50} value of each compound was calculated using GraphPad Prism 5.0.

Cell-Cycle Assay and Cell Apoptosis. MCF7 and HepG2 cells were plated in 6-well plates and treated with each compound (1 μM) for 24 h. For the cell-cycle assay, the cells were washed twice with ice-cold PBS, treated with ice-cold 70% ethanol while being vortexed, and fixed overnight at 4 °C. After being centrifuged for 5 min at 1000g, the cells were washed with 1 mL of ice-cold PBS and stained with 0.5 mL of a mixture containing 465 μL of 1× PBS, 25 μL of propidium iodide (PI), and 10 μL of RNaseA at 37 °C for 30 min. The data were collected using an Attune NxT Acoustic Focusing Cytometer (Life Technologies) and analyzed using the ModFit LT software (Verity Software House, Inc.).

For the cell-apoptosis analysis, the cells were collected and suspended in 0.5 mL of 1× binding buffer and washed twice with ice-cold PBS. The annexin V−FITC Apoptosis Detection Kit (Vazyme) was used according to the manufacturer's instructions for the apoptosis assay. The stained cells were analyzed by a BD Accuri C6 Plus flow cytometer equipped with the BD Accuri C6 Software (Becton Dickinson).

Western Blot. The cells were washed twice with PBS and extracted using 1% Nonidet P-40, 50 mM Tris-HCl (pH 8.0), 150 mM NaCl, 0.5% sodium deoxycholate, 1 mM phenyl methyl sulfonyl fluoride, 1 mM Na_3VO_4, 1 mM NaF, and protease inhibitors (Roche). The protein lysates (25 μg) were separated by SDS-PAGE and transferred onto PVDF membranes (Merck Millipore). After being blocked, the membranes were incubated at 4 °C overnight with the following primary antibodies: anti-VDR (1:1000, Santa Cruz Biotechnology), anti-p21 (1:500, Bioworld), anti-p27 (1:500, Santa Cruz Biotechnology) and anti-β-actin (1:5000, Cell Signaling Technology).

Cellular Uptake and Metabolic Stability. For the measurement of the cellular uptake of the compounds, MCF7 cells were plated in 12-well plates at a density 2×10^5 cells/well. After being incubated for 24 h, the cells were incubated again with 1 μM calcitriol, sw22, LG190119, **11b**, **11d**, or **11g** for 10 or 30 min. After the incubations, each compound was extracted from the cells and medium separately using three volumes of chloroform/methanol (3:1, v/v). The organic phase was recovered and dried under reduced pressure. The residue was dissolved in acetonitrile and applied to HPLC for analysis. To estimate the stabilities of the compounds in the culture medium, MCF7 cells plated in 12-well plates at a density of 2×10^5 cells/well were incubated with 1 μM calcitriol, sw22, LG190119, **11b**, **11d**, or **11g** for 24 h. After the incubation, each compound was extracted using three volumes of chloroform/methanol (3:1, v/v) from the cells and medium together. After the organic phase was evaporated, the residue was dissolved in acetonitrile and applied to an HPLC for analysis.

In Vivo Calcemic-Activity Assay. ICR mice (obtained from Shanghai Silaike Laboratory Animal Ltd., 7 weeks, 18−22 g) were housed under normal lighting and received a vitamin D deficient, calcium-replete diet (0.2% calcium, 1% phosphorus, 2000 units of vitamins) and water for 7 days prior to being treated with various concentrations of the compounds. The compounds, dissolved in ethanol/polyoxyethylenated castor oil (EL)/saline (1:1:18), were injected intraperitoneally daily for 7 days. The mice fasted overnight, and venous blood was withdrawn on the eighth day. Then, the total calcium-ion concentration in the venous blood was colorimetrically determined by the methyl timolol blue (MTB) method using a calcium-assay kit (Nanjing Jiancheng Bioengineering Institute).

In Vivo Antitumor-Activity Assay. Female BALB/c nude mice weighing approximately 20 g were obtained from the Beijing Vital River Laboratory Animal Technology Company Ltd. (Beijing, China). To generate the MCF7-tumor-bearing mouse model, 1×10^7 cells were inoculated in the left, fourth mammary fat pads of the nude mice. Upon reaching average tumor volumes of 50 mm^3 (7 days after the injections), the animals were randomly divided into eight groups: (1) saline, (2) vehicle, (3) calcitriol, (4) sw22, (5) LG190119, (6) **11b**, (7) **11d**, and (8) **11g** (n = 7). The sw22, LG190119, **11b**, **11d**, and **11g** groups (10 mg/kg, prepared in ethanol/EL/saline = 1:1:18); the calcitriol group (0.5 μg/kg, prepared in ethanol/EL/saline = 1:1:18); the vehicle group (ethanol/EL/saline = 1:1:18); and the saline group were given intraperitoneal injections every other day. The body weights were also monitored every other day during the experiments. The tumor volumes were measured periodically throughout the experiments using a digital caliper, and the tumor volume was calculated by the following formula: tumor volume (mm^3) = (L × W × W)/2, where L is the length in millimeters and W is the width in millimeters. One day after the last injection, blood was collected, and the calcium-ion concentrations were determined using a calcium-assay kit. Then, the tumors were collected from the euthanized mice and washed with saline several times. Furthermore, immunohistochemistry of Ki-67 was performed on paraffin sections by using rabbit anti-mouse-Ki-67 (1:200, Cell Signaling Technology) and staining with the HRP-DAB SPlink Detection Kit (ZSGB-Bio). Apoptosis in the tumors was evaluated by TUNEL staining using an In Situ Cell Death Detection Kit (Roche) according to the manufacturer's protocol. The Ki-67 staining and TUNEL staining were photographed using a Microscope BX53 (Olympus) and analyzed by ImageJ 1.51n with the ImmunoRatio 1.0 c plugin. The Animal Care and Use Committee of the China Pharmaceutical University approved all of the animal studies and animal protocols.

Pharmacokinetics Study. Compounds **11b** and **11g** were dissolved in ethanol/EL/saline (1:1:18) for the intraperitoneal and intravenous injections or in ethanol/medium-chain triglycerides (MCT, 1:9) for the oral administration. Male Sprague-Dawley (SD) rats weighing 180−220 g were injected intravenously with 5 mg/kg doses, injected intraperitoneally with 20 mg/kg doses, or given 20 mg/kg doses orally (n = 4). After the administration, blood samples were collected from the posterior orbital venous plexus at 5.0, 15, and 30 min and at 1.0, 2.0, 4.0, 6.0, 8.0, 12.0, 24.0, and 48.0 h and then immediately centrifuged (12 000 rpm, 10 min) to obtain plasma samples. The compounds in the plasma samples were extracted with acetonitrile and stored at −20 °C until they were tested by HPLC to measure the concentrations. The pharmacokinetic parameters were calculated by Kinetica 4.4 software.

DOI: 10.1021/acs.jmedchem.8b00106
J. Med. Chem. 2018, 61, 3059−3075

Statistical Analysis. Data were presented as the means ± SEM from at least three independent experiments. Student's unpaired *t* test was used for two-group comparisons in the appropriate conditions. ***$p < 0.001$, **$p < 0.01$, *$p < 0.05$.

■ ASSOCIATED CONTENT

Supporting Information

The Supporting Information is available free of charge on the ACS Publications website at DOI: 10.1021/acs.jmedchem.8b00106.

Biological data; procedures for the preparation of the intermediates; and ^{1}H NMR, ^{13}C NMR, and HRMS spectra of the phenyl-pyrrolyl pentane derivatives (PDF)
Molecular-formula strings for the studied compounds (CSV)

■ AUTHOR INFORMATION

Corresponding Author

*E-mail: zhangcan@cpu.edu.cn.

ORCID

Meixi Hao: 0000-0002-2049-2220

Haoliang Yuan: 0000-0003-0248-4347

Author Contributions

†M.H. and S.H. contributed equally to this work. The manuscript was written through contributions of all authors. All authors have given approval to the final version of the manuscript.

Notes

The authors declare no competing financial interest.

■ ACKNOWLEDGMENTS

We thank the Public Platform of the State Key Laboratory of Natural Medicines for assistance with the pathological-section imaging, and we are grateful to Yumeng Shen and Ping Zhou for their help in analyzing images. This work was supported by the National Natural Science Foundation of China (81273468 and 81473153), the National Basic Research Program of China (2015CB755500), and the 111 Project from the Ministry of Education of China and the State Administration of Foreign Expert Affairs of China (No. 111-2-07).

■ ABBREVIATIONS USED

VDR, vitamin D receptor; EC_{50}, half-maximum (50%) effective concentration of a substance; MTT, 3-(4,5-dimethyl-2-thiazolyl)-2,5-diphenyl-2-*H*-tetrazolium bromide; IC_{50}, half-maximum (50%) inhibitory concentration of a substance; PK, pharmacokinetic; LBD, ligand-binding domain; TMS, tetramethylsilane; HRMS, high-resolution mass spectra; TLC, thin-layer chromatography; UV, ultraviolet light; DMF, *N*,*N*-dimethylformamide; FBS, fetal bovine serum; DMEM, Dulbecco's Modified Eagle's Medium; NEAA, nonessential amino acid; NBT, nitroblue tetrazolium; TPA, 12-*O*-tetradecanoylphorbol-13-acetate; PI, propidium iodide; MCT, medium-chain triglycerides; EL, polyoxyethylenated castor oil

■ REFERENCES

(1) Deeb, K. K.; Trump, D. L.; Johnson, C. S. Vitamin D signalling pathways in cancer: potential for anticancer therapeutics. *Nat. Rev. Cancer* **2007**, *7*, 684−700.

(2) Plum, L. A.; DeLuca, H. F. Vitamin D, disease and therapeutic opportunities. *Nat. Rev. Drug Discovery* **2010**, *9*, 941−955.

(3) Khanal, R.; Nemere, I. Membrane receptors for vitamin D metabolites. *Crit. Rev. Eukaryotic Gene Expression* **2007**, *17*, 31−47.

(4) Feldman, D.; Krishnan, A. V.; Swami, S.; Giovannucci, E.; Feldman, B. J. The role of vitamin D in reducing cancer risk and progression. *Nat. Rev. Cancer* **2014**, *14*, 342−357.

(5) Sherman, M. H.; Yu, R. T.; Engle, D. D.; Ding, N.; Atkins, A. R.; Tiriac, H.; Collisson, E. A.; Connor, F.; Van Dyke, T.; Kozlov, S.; Martin, P.; Tseng, T. W.; Dawson, D. W.; Donahue, T. R.; Masamune, A.; Shimosegawa, T.; Apte, M. V.; Wilson, J. S.; Ng, B.; Lau, S. L.; Gunton, J. E.; Wahl, G. M.; Hunter, T.; Drebin, J. A.; O'Dwyer, P. J.; Liddle, C.; Tuveson, D. A.; Downes, M.; Evans, R. M. Vitamin D receptor-mediated stromal reprogramming suppresses pancreatitis and enhances pancreatic cancer therapy. *Cell* **2014**, *159*, 80−93.

(6) Garland, C. F.; Comstock, G. W.; Garland, F. C.; Helsing, K. J.; Shaw, E. K.; Gorham, E. D. Serum 25-hydroxyvitamin D and colon cancer: eight-year prospective study. *Lancet* **1989**, *334*, 1176−1178.

(7) Carballa, D. M.; Seoane, S.; Zacconi, F.; Perez, X.; Rumbo, A.; Alvarez-Diaz, S.; Larriba, M. J.; Perez-Fernandez, R.; Munoz, A.; Maestro, M.; Mourino, A.; Torneiro, M. Synthesis and biological evaluation of 1 alpha,25-Dihydroxyvitamin D-3 Analogues with a Long Side Chain at C12 and Short C17 Side Chains. *J. Med. Chem.* **2012**, *55*, 8642−8656.

(8) Berger, U.; McClelland, R. A.; Wilson, P.; Greene, G. L.; Haussler, M. R.; Pike, J. W.; Colston, K.; Easton, D.; Coombes, R. C. Immunocytochemical determination of estrogen receptor, progesterone receptor, and 1,25-dihydroxyvitamin D3 receptor in breast cancer and relationship to prognosis. *Cancer Res.* **1991**, *51*, 239−244.

(9) Bertone-Johnson, E. R.; Chen, W. Y.; Holick, M. F.; Hollis, B. W.; Colditz, G. A.; Willett, W. C.; Hankinson, S. E. Plasma 25-hydroxyvitamin D and 1,25-dihydroxyvitamin D and risk of breast cancer. *Cancer Epidemiol., Biomarkers Prev.* **2005**, *14*, 1991−1997.

(10) Hendrickson, W. K.; Flavin, R.; Kasperzyk, J. L.; Fiorentino, M.; Fang, F.; Lis, R.; Fiore, C.; Penney, K. L.; Ma, J.; Kantoff, P. W.; Stampfer, M. J.; Loda, M.; Mucci, L. A.; Giovannucci, E. Vitamin D receptor protein expression in tumor tissue and prostate cancer progression. *J. Clin. Oncol.* **2011**, *29*, 2378−2385.

(11) Ahonen, M. H.; Tenkanen, L.; Teppo, L.; Hakama, M.; Tuohimaa, P. Prostate cancer risk and prediagnostic serum 25-hydroxyvitamin D levels (Finland). *Cancer Causes Control* **2000**, *11*, 847−852.

(12) Bao, Y.; Ng, K.; Wolpin, B. M.; Michaud, D. S.; Giovannucci, E.; Fuchs, C. S. Predicted vitamin D status and pancreatic cancer risk in two prospective cohort studies. *Br. J. Cancer* **2010**, *102*, 1422−1427.

(13) Erber, E.; Maskarinec, G.; Lim, U.; Kolonel, L. N. Dietary vitamin D and risk of non-Hodgkin lymphoma: the multiethnic cohort. *Br. J. Nutr.* **2010**, *103*, 581−584.

(14) Zinser, G. M.; Sundberg, J. P.; Welsh, J. Vitamin D(3) receptor ablation sensitizes skin to chemically induced tumorigenesis. *Carcinogenesis* **2002**, *23*, 2103−2109.

(15) Garland, C. F.; Garland, F. C. Do sunlight and vitamin D reduce the likelihood of colon cancer? *Int. J. Epidemiol* **1980**, *9*, 227−231.

(16) Lappe, J. M.; Travers-Gustafson, D.; Davies, K. M.; Recker, R. R.; Heaney, R. P. Vitamin D and calcium supplementation reduces cancer risk: results of a randomized trial. *Am. J. Clin. Nutr.* **2007**, *85*, 1586−1591.

(17) Dalhoff, K.; Dancey, J.; Astrup, L.; Skovsgaard, T.; Hamberg, K. J.; Lofts, F. J.; Rosmorduc, O.; Erlinger, S.; Bach Hansen, J.; Steward, W. P.; Skov, T.; Burcharth, F.; Evans, T. R. A phase II study of the vitamin D analogue seocalcitol in patients with inoperable hepatocellular carcinoma. *Br. J. Cancer* **2003**, *89*, 252−257.

(18) Srinivas, S.; Feldman, D. A phase II trial of calcitriol and naproxen in recurrent prostate cancer. *Anticancer Res.* **2009**, *29*, 3605−3610.

(19) Beer, T. M.; Ryan, C. W.; Venner, P. M.; Petrylak, D. P.; Chatta, G. S.; Ruether, J. D.; Redfern, C. H.; Fehrenbacher, L.; Saleh, M. N.; Waterhouse, D. M.; Carducci, M. A.; Vicario, D.; Dreicer, R.; Higano, C. S.; Ahmann, F. R.; Chi, K. N.; Henner, W. D.; Arroyo, A.; Clow, F. W. Double-blinded randomized study of high-dose calcitriol plus docetaxel compared with placebo plus docetaxel in androgen-

DOI: 10.1021/acs.jmedchem.8b00106
J. Med. Chem. 2018, 61, 3059−3075

independent prostate cancer: a report from the ASCENT Investigators. *J. Clin. Oncol.* **2007**, *25*, 669−674.
(20) Leyssens, C.; Verlinden, L.; Verstuyf, A. The future of vitamin D analogs. *Front. Physiol.* **2014**, *5*, 122.
(21) Christakos, S.; Dhawan, P.; Verstuyf, A.; Verlinden, L.; Carmeliet, G. Vitamin D: metabolism, molecular mechanism of action, and pleiotropic effects. *Physiol. Rev.* **2016**, *96*, 365−408.
(22) Galsky, M. D.; Vogelzang, N. J. Docetaxel-based combination therapy for castration-resistant prostate cancer. *Ann. Oncol* **2010**, *21*, 2135−2144.
(23) Gross, C.; Stamey, T.; Hancock, S.; Feldman, D. Treatment of early recurrent prostate cancer with 1,25-dihydroxyvitamin D3 (calcitriol). *J. Urol.* **1998**, *159*, 2035−2039.
(24) Polek, T. C.; Murthy, S.; Blutt, S. E.; Boehm, M. F.; Zou, A.; Weigel, N. L.; Allegretto, E. A. Novel nonsecosteroidal vitamin D receptor modulator inhibits the growth of LNCaP xenograft tumors in athymic mice without increased serum calcium. *Prostate* **2001**, *49*, 224−233.
(25) Watarai, Y.; Ishizawa, M.; Ikura, T.; Zacconi, F. C. M.; Uno, S.; Ito, N.; Mourino, A.; Tokiwa, H.; Makishima, M.; Yamada, S. Synthesis, biological activities, and X-ray crystal structural analysis of 25-Hydroxy-25(or 26)-adamantyl-17420(22),23-diynyl]-21-norvitamin D compounds. *J. Med. Chem.* **2015**, *58*, 9510−9521.
(26) Boehm, M. F.; Fitzgerald, P.; Zou, A.; Elgort, M. G.; Bischoff, E. D.; Mere, L.; Mais, D. E.; Bissonnette, R. P.; Heyman, R. A.; Nadzan, A. M.; Reichman, M.; Allegretto, E. A. Novel nonsecosteroidal vitamin D mimics exert VDR-modulating activities with less calcium mobilization than 1,25-dihydroxyvitamin D3. *Chem. Biol.* **1999**, *6*, 265−275.
(27) Fujii, S.; Masuno, H.; Taoda, Y.; Kano, A.; Wongmayura, A.; Nakabayashi, M.; Ito, N.; Shimizu, M.; Kawachi, E.; Hirano, T.; Endo, Y.; Tanatani, A.; Kagechika, H. Boron cluster-based development of potent nonsecosteroidal vitamin D receptor ligands: direct observation of hydrophobic interaction between protein surface and carborane. *J. Am. Chem. Soc.* **2011**, *133*, 20933−20941.
(28) Ciesielski, F.; Sato, Y.; Chebaro, Y.; Moras, D.; Dejaegere, A.; Rochel, N. Structural basis for the accommodation of bis- and tris-aromatic derivatives in vitamin D nuclear receptor. *J. Med. Chem.* **2012**, *55*, 8440−8449.
(29) Ma, Y.; Khalifa, B.; Yee, Y. K.; Lu, J.; Memezawa, A.; Savkur, R. S.; Yamamoto, Y.; Chintalacharuvu, S. R.; Yamaoka, K.; Stayrook, K. R.; Bramlett, K. S.; Zeng, Q. Q.; Chandrasekhar, S.; Yu, X. P.; Linebarger, J. H.; Iturria, S. J.; Burris, T. P.; Kato, S.; Chin, W. W.; Nagpal, S. Identification and characterization of noncalcemic, tissue-selective, nonsecosteroidal vitamin D receptor modulators. *J. Clin. Invest.* **2006**, *116*, 892−904.
(30) Tavera-Mendoza, L. E.; Quach, T. D.; Dabbas, B.; Hudon, J.; Liao, X.; Palijan, A.; Gleason, J. L.; White, J. H. Incorporation of histone deacetylase inhibition into the structure of a nuclear receptor agonist. *Proc. Natl. Acad. Sci. U. S. A.* **2008**, *105*, 8250−8255.
(31) Shen, W.; Xue, J.; Zhao, Z.; Zhang, C. Novel nonsecosteroidal VDR agonists with phenyl-pyrrolyl pentane skeleton. *Eur. J. Med. Chem.* **2013**, *69*, 768−778.
(32) Ge, Z.; Hao, M.; Xu, M.; Su, Z.; Kang, Z.; Xue, L.; Zhang, C. Novel nonsecosteroidal VDR ligands with phenyl-pyrrolyl pentane skeleton for cancer therapy. *Eur. J. Med. Chem.* **2016**, *107*, 48−62.
(33) Gill, H. S.; Londowski, J. M.; Corradino, R. A.; Zinsmeister, A. R.; Kumar, R. The synthesis and biological activity of 25-hydroxy-26,27-dimethylvitamin D3 and 1,25-dihydroxy-26,27-dimethylvitamin D3: highly potent novel analogs of vitamin D3. *J. Steroid Biochem.* **1988**, *31*, 147−160.
(34) Wang, B.; Hao, M. X.; Zhang, C. Design, synthesis and biological evaluation of nonsecosteroidal vitamin D-3 receptor ligands as anti-tumor agents. *Bioorg. Med. Chem. Lett.* **2017**, *27*, 1428−1436.
(35) Binderup, L.; Latini, S.; Binderup, E.; Bretting, C.; Calverley, M.; Hansen, K. 20-epi-vitamin D3 analogues: a novel class of potent regulators of cell growth and immune responses. *Biochem. Pharmacol.* **1991**, *42*, 1569−1575.
(36) Chesney, R. W.; Han, X. Differential regulation of TauT by calcitriol and retinoic acid via VDR/RXR in LLC-PK1 and MCF-7 cells. *Adv. Exp. Med. Biol.* **2013**, *776*, 291−305.
(37) Yin, Y.; Ni, J.; Chen, M.; Guo, Y. L.; Yeh, S. Y. RRR-alpha-Vitamin E succinate potentiates the antitumor effect of calcitriol in prostate cancer without overt side effects. *Clin. Cancer Res.* **2009**, *15*, 190−200.
(38) Larriba, M. J.; Munoz, A. SNAIL vs vitamin D receptor expression in colon cancer: therapeutics implications. *Br. J. Cancer* **2005**, *92*, 985−989.
(39) Chiang, K. C.; Yeh, C. N.; Chen, H. Y.; Lee, J. M.; Juang, H. H.; Chen, M. F.; Takano, M.; Kittaka, A.; Chen, T. C. 19-Nor-2alpha-(3-hydroxypropyl)-1alpha,25-dihydroxyvitamin D3 (MART-10) is a potent cell growth regulator with enhanced chemotherapeutic potency in liver cancer cells. *Steroids* **2011**, *76*, 1513−1519.
(40) Haussler, M. R.; McCain, T. A. Basic and clinical concepts related to vitamin D metabolism and action (first of two parts). *N. Engl. J. Med.* **1977**, *297*, 974−983.
(41) Maruyama, K.; Noguchi-Yachide, T.; Sugita, K.; Hashimoto, Y.; Ishikawa, M. Novel selective anti-androgens with a diphenylpentane skeleton. *Bioorg. Med. Chem. Lett.* **2010**, *20*, 6661−6666.
(42) Thomas, E.; Brion, J. D.; Peyrat, J. F. Synthesis and preliminary biological evaluation of new antiproliferative aromatic analogues of 1alpha,25-dihydroxyvitamin D3. *Eur. J. Med. Chem.* **2014**, *86*, 381−393.
(43) Kakuda, S.; Okada, K.; Eguchi, H.; Takenouchi, K.; Hakamata, W.; Kurihara, M.; Takimoto-Kamimura, M. Structure of the ligand-binding domain of rat VDR in complex with the nonsecosteroidal vitamin D3 analogue YR301. *Acta Crystallogr., Sect. F: Struct. Biol. Cryst. Commun.* **2008**, *64*, 970−973.
(44) Yamada, S.; Makishima, M. Structure-activity relationship of nonsecosteroidal vitamin D receptor modulators. *Trends Pharmacol. Sci.* **2014**, *35*, 324−337.
(45) Ciesielski, F.; Rochel, N.; Mitschler, A.; Kouzmenko, A.; Moras, D. Structural investigation of the ligand binding domain of the zebrafish VDR in complexes with 1alpha,25(OH)2D3 and Gemini: purification, crystallization and preliminary X-ray diffraction analysis. *J. Steroid Biochem. Mol. Biol.* **2004**, *89*−*90*, 55−59.
(46) Jensen, S. S.; Madsen, M. W.; Lukas, J.; Binderup, L.; Bartek, J. Inhibitory effects of 1alpha,25-dihydroxyvitamin D(3) on the G(1)-S phase-controlling machinery. *Mol. Endocrinol.* **2001**, *15*, 1370−1380.
(47) Caputo, A.; Pourgholami, M. H.; Akhter, J.; Morris, D. L. 1,25-Dihydroxyvitamin D(3) induced cell cycle arrest in the human primary liver cancer cell line HepG2. *Hepatol. Res.* **2003**, *26*, 34−39.
(48) Flores, O.; Wang, Z.; Knudsen, K. E.; Burnstein, K. L. Nuclear targeting of cyclin-dependent kinase 2 reveals essential roles of cyclin-dependent kinase 2 localization and cyclin E in vitamin D-mediated growth inhibition. *Endocrinology* **2010**, *151*, 896−908.
(49) Swami, S.; Krishnan, A. V.; Wang, J. Y.; Jensen, K.; Peng, L.; Albertelli, M. A.; Feldman, D. Inhibitory effects of calcitriol on the growth of MCF-7 breast cancer xenografts in nude mice: selective modulation of aromatase expression in vivo. *Horm. Cancer* **2011**, *2*, 190−202.
(50) Yoon, I. S.; Son, J. H.; Kim, S. B.; Choi, M. K.; Maeng, H. J. Effects of 1alpha,25-Dihydroxyvitamin D3 on Intestinal Absorption and Disposition of Adefovir Dipivoxil and Its Metabolite, Adefovir, in Rats. *Biol. Pharm. Bull.* **2015**, *38*, 1732−1737.
(51) Choi, M.; Yamada, S.; Makishima, M. Dynamic and ligand-selective interactions of vitamin D receptor with retinoid X receptor and cofactors in living cells. *Mol. Pharmacol.* **2011**, *80*, 1147−1155.
(52) Ohyama, Y.; Ozono, K.; Uchida, M.; Shinki, T.; Kato, S.; Suda, T.; Yamamoto, O.; Noshiro, M.; Kato, Y. Identification of a vitamin D-responsive element in the 5′-flanking region of the rat 25-hydroxyvitamin D3 24-hydroxylase gene. *J. Biol. Chem.* **1994**, *269*, 10545−10550.
(53) Kim, S.; Shevde, N. K.; Pike, J. W. 1,25-Dihydroxyvitamin D3 stimulates cyclic vitamin D receptor/retinoid X receptor DNA-binding, co-activator recruitment, and histone acetylation in intact osteoblasts. *J. Bone Miner. Res.* **2005**, *20*, 305−317.

DOI: 10.1021/acs.jmedchem.8b00106
J. Med. Chem. 2018, 61, 3059−3075

(54) Issa, L. L.; Leong, G. M.; Sutherland, R. L.; Eisman, J. A. Vitamin D analogue-specific recruitment of vitamin D receptor coactivators. *J. Bone Miner. Res.* **2002**, *17*, 879−890.
(55) Masuda, S.; Jones, G. Promise of vitamin D analogues in the treatment of hyperproliferative conditions. *Mol. Cancer Ther.* **2006**, *5*, 797−808.
(56) Scher, H. I.; Jia, X.; Chi, K.; de Wit, R.; Berry, W. R.; Albers, P.; Henick, B.; Waterhouse, D.; Ruether, D. J.; Rosen, P. J.; Meluch, A. A.; Nordquist, L. T.; Venner, P. M.; Heidenreich, A.; Chu, L.; Heller, G. Randomized, open-label phase III trial of docetaxel plus high-dose calcitriol versus docetaxel plus prednisone for patients with castration-resistant prostate cancer. *J. Clin. Oncol.* **2011**, *29*, 2191−2198.

DOI: 10.1021/acs.jmedchem.8b00106
J. Med. Chem. 2018, 61, 3059−3075